GLIOMA CHEMOTHERAPY SENSITIZATION MEDIATED BY BASE EXCISION REPAIR INHIBITION AND ITS POTENTIAL APPLICATION

by

Jiangbo Tang

B.S., Wuhan University, 2001

Submitted to the Graduate Faculty of

Graduate School of Public Health in partial fulfillment

of the requirements for the degree of

Doctor of Philosophy

University of Pittsburgh

2010

UNIVERSITY OF PITTSBURGH

Graduate School of Public Health

This thesis was presented

by

Jiangbo Tang

It was defended on

March 1, 2010

and approved by

Dissertation Advisor
Robert W. Sobol, Ph.D.
Assistant Professor, Department of Pharmacology & Chemical Biology
School of Medicine, University of Pittsburgh

Robert E. Ferrell, Ph.D.,
Professor, Department of Human Genetics
Graduate School of Public Health, University of Pittsburgh

Susanne M. Gollin, Ph.D.
Professor, Department of Human Genetics
Graduate School of Public Health, University of Pittsburgh

Lin Zhang, Ph.D.
Associate Professor, Department of Pharmacology & Chemical Biology
School of Medicine, University of Pittsburgh

**GLIOMA CHEMOTHERAPY SENSITIZATION MEDIATED BY BASE EXCISION
REPAIR INHIBITION AND ITS POTENTIAL APPLICATION**

Jiangbo Tang, Ph.D.

University of Pittsburgh, 2010

The incidence and mortality of brain tumors have not changed over the last 3 decades and pose a significant burden on the healthcare system of the United States. Temozolomide (TMZ) is the preferred chemotherapeutic agent for the treatment of brain tumors and base excision repair (BER) is a major mechanism for the repair of TMZ-induced DNA base lesions. BER inhibition, either by interrupting the delicate balance of the expression of key BER proteins or by chemical inhibitors, enhances cytotoxicity of chemotherapeutic DNA damaging agents such as TMZ. Understanding the mechanisms of enhanced cytotoxicity brought on by BER inhibition has great public health significance.

By using DNA polymerase ß (Polß) deficiency as a model of BER inhibition, I report that DNA damage-induced cytotoxicity due to Polß deficiency triggers cell death dependent on PARP activation yet independent of poly(ADP-ribose) (PAR) or PAR-catabolite signaling. Cell death is rescued by the NAD^+ metabolite NMN and is synergistic with inhibition of NAD^+ biosynthesis demonstrating that DNA damage-induced cytotoxicity mediated via BER inhibition is primarily dependent on cellular metabolite bioavailability. I offer a mechanistic justification for the elevated alkylation-induced cytotoxicity of Polß deficient cells, suggesting a linkage between DNA repair, cell survival and cellular bioenergetics.

Resistance to TMZ is partially attributed to efficient repair of TMZ-induced DNA lesions. Using the human glioma cell lines LN428 and T98G, I report here that potentiation of TMZ via BER inhibition (methoxyamine (MX), the PARP inhibitors PJ34 and ABT-888 or depletion (knockdown) of PARG) is greatly enhanced by increasing BER initiation via over-expression of MPG. I also show that MX-induced potentiation of TMZ in MPG expressing glioma cells is abrogated by elevated-expression of the rate-limiting BER enzyme Polß, suggesting that cells proficient for BER readily repair AP sites even in the presence of MX. This study demonstrates that increased initiation of BER via MPG over-expression, together with inhibition of repair following initiation, further sensitizes glioma cells to alkylating agent TMZ, suggesting that the expression level of MPG might be used to predict the effectiveness of BER inhibition-induced potentiation of TMZ in glioma cells.

TABLE OF CONTENTS

LIST OF TABLES

LIST OF FIGURES

LIST OF ABBREVIATIONS

BER   base excision repair

Polß   DNA polymerase ß

TMZ   temozolomide

PARP1   poly(ADP-ribose) polymerase 1

PARP2   poly(ADP-ribose) polymerase 2

PARP   poly(ADP-ribose) polymerase

MEFs   mouse embryonic fibroblasts

MPG   N-methylpurine DNA glycosylase

MX   methoxyamine

CNS   central nervous system

PNETs   primitive neuroectodermal tumors

GBM   glioblastoma multiforme

EGFR   epidermal growth factor receptor

cdk4   cyclin-dependent kinase 4

cdk6   cyclin-dependent kinase 6

Rb   retinoblastoma

BCNU   carmustine, bichloroethyl nitrosourea

CCNU   lomustine, chloroethylnitrosourea

7MeG	N7-methylguanine
3MeA	N3-methyladenine
O^6MeG	O^6-methylguanine
MMR	mismatch repair
MGMT	O^6-methylguanine-DNA methyltransferase
APE1	apurinic/apyrimidinic endonuclease 1
5'dRP	5'deoxyribose phosphate
FEN1	Flap endonuclease 1
LIGI	DNA Ligase I
LIGIIIα	DNA Ligase IIIα
XRCC1	X-ray repair cross complementing protein 1
AIF	apoptosis inducing factor
WT	wild type
SSBs	single-stranded DNA breaks
DSBs	DNA double-stranded breaks
HR	homologous recombination
PARG	poly(ADP-ribose) glycohydrolase
RIP	receptor-interacting protein 1
AAG	alkyladenine DNA glycosylase
PARP2	poly(ADP-ribose) polymerase 2
FBS	fetal bovine serum
DMSO	dimethyl sulfoxide
MMS	methyl methanesulfonate

MNNG	*N*-Methyl-*N*'-Nitro-*N*-Nitrosoguanidine
NMN	ß-nicotinamide mononucleotide
NA	Nicotinic Acid
FACS	fluorescence-activated cell sorting
HRP	horseradish peroxidase
ES	embryonic stem
NAMPT	nicotinamide phosphoribosyltransferase

PREFACE

I am grateful to all the people who generously provided their help and support that made my Ph.D. thesis research possible.

Dr. Robert Sobol has been an extremely responsible, supportive, and intelligent mentor. I would like to thank him for his valuable guidance throughout my Ph.D. thesis research. I would also like to thank my committee members, Dr. Robert Ferrell, Dr. Susan Gollin, and Dr. Lin Zhang for their insightful discussions and inputs. They have always been supportive and helpful.

I am indebted to the Department of Human Genetics at the University of Pittsburgh. I received my Ph.D. study admission in 2003 from the department. Unfortunately, I could not join the department until the beginning of 2005. If it were not the continuous support from the department, my Ph.D. training at the University of Pittsburgh would not come true.

At the University of Pittsburgh Cancer Institute, I am lucky to work with a group of great scientists in the field of DNA repair research. They shared their vast experiences with me and helped me build a solid understanding of almost all areas of DNA repair research. Thanks to Dr. Rick Wood, Dr. Christopher Bakkenist, Dr. Laura Niedernhofer, Dr. Bennett Van Houten, Dr. Patricia Opresko, and Dr. Yong Wan. My sincerest thanks to Dr. Jay White for his help and all the discussions I had with him.

I would also like to thank the members of the Sobol lab, Dr. Ram Trivedi, Dr. Elena Jelezcova, Xiao-hong Wang, Eva Goellner, Ashley Brown, David Svilar, and Stacy Lin. They provided enormous help when I first started and throughout my Ph.D. study.

I dedicate this thesis to my wife, Qi, and our daughter, Claire.

1.0   STATEMENT OF THE PROBLEM

Efficacy of chemotherapy or radiation treatment is intimately dependent on DNA repair capacity. Base excision repair (BER) is one of the major mechanisms conferring resistance to DNA damage-induced cytotoxicity. The mechanism of enhanced cytotoxicity of chemotherapeutic DNA-damaging agents via BER inhibition and the methodologies to improve chemotherapy efficacy are of great importance from both public health and clinical perspectives.

The BER pathway repairs DNA base lesions through the assembly and coordinated function of a series of repair complexes at the site of the DNA lesion. The expression of BER proteins is under cellular regulation to ensure coordinated function of the components of the repair complexes. An imbalance of BER protein expression, for example DNA polymerase ß (Polß) deficiency, is a form of BER inhibition that enhances cytotoxicity of radiation and chemotherapeutic DNA-damaging agents. Despite recent progress that has been made to elucidate the mechanism of BER inhibition-induced sensitization, the signaling pathways and cell death mediators that lead to increased cytotoxicity remain unknown.

Temozolomide (TMZ) is the preferred chemotherapeutic alkylating agent in the treatment of glioma following surgical resection and/or radiation. One mechanism of resistance to TMZ is attributed to efficient repair of TMZ-induced DNA lesions by the BER pathway. It has been shown that increased repair initiation of the BER pathway provides enhanced cytotoxicity of cancer cells to TMZ. However, it is not clear if increased repair initiation can be combined with

inhibition of repair steps following repair initiation to achieve further sensitization of cancer

cells.

2.0   SPECIFIC AIMS

Specific Aim 1: To determine if poly(ADP-ribose) polymerase 1 (PARP1) mediates cell death in response to BER inhibition. In the absence of the BER rate-limiting enzyme Polß, cellular hypersensitivity to alkylating agents have been observed in mouse embryonic fibroblasts (MEFs), in human cancer cells and in animal models. Although the cellular hypersensitivity is known to be due to the accumulation of BER intermediates resulting from incomplete repair, the exact downstream signaling process leading to cell death is unclear. **I propose that PARP1 functions in BER as a molecular sensor, signaling in response to the inhibition of BER and leading to cellular energy depletion-dependent cell death.** To address this hypothesis the following experiments are proposed: A) Correlate enzymatic activation of PARP1 with inhibition of the BER pathway. B) Determine the functional significance of PARP1 activation in controlling short-term survival of cells following BER inhibition. C) Determine the specific cell death mechanisms that are activated following PARP1 activation.

Specific Aim 2: To test the hypothesis that increased repair initiation enhances BER inhibition-mediated sensitization of glioma cells to TMZ. Increased repair initiation via over-expression of the BER initiating enzyme N-methylpurine DNA glycosylase (MPG) has been reported to sensitize human breast cancer cells, osteosarcoma cells, and ovarian cancer cells to TMZ. Enhanced sensitivity to alkylating agents have also been observed by inhibition of the

BER pathway in preclinical studies, suggesting BER modulation is an attractive strategy for chemotherapy potentiation. **I propose that BER inhibition-induced sensitization is dependent on BER initiation and increased repair initiation can be combined with BER inhibition to further increase efficacy of alkylation treatment.** To address this hypothesis, I propose the following experiments. A) Determine if methoxyamine (MX)-induced sensitization of glioma cells to TMZ can be enhanced by increased initiation of BER. B) Assay if depletion of PARG and the resulting potentiation of TMZ can be increased by elevated repair initiation. C) Assess if inhibition of PARP-induced sensitization of TMZ can be enhanced by increased repair initiation.

3.0   INTRODUCTION

3.1   GLIOMA AND CHEMOTHERPAY

3.1.1 Brain tumors and glioma
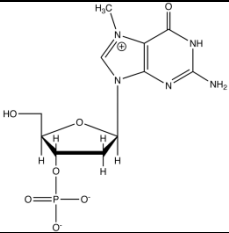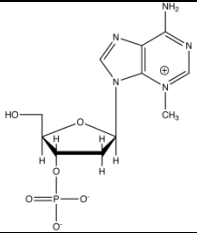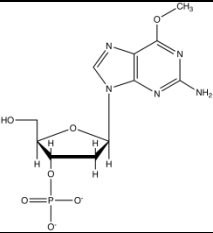
Neoplastic transformation in the central nervous system (CNS) is a multistep process involving cellular and genetic alterations and the interaction between those alterations and environmental factors (1). Primary benign and malignant brain tumors are common. It is the second most common cancer and the most common solid tumor in childhood (1). The incidence of primary brain and CNS tumors has remained at a similar level over the last 3 decades (2). The overall incidence rate for 2004-2005 was 18.16 per 100,000 person-years. The overall incidence rate was 4.58 per 100,000 person-years for children 0-19 years of age and 23.62 per 100,000 person-years for adults (20+ years) (2). Glial tumors, primitive neuroectodermal tumors (PNETs), meningiomas, and schwannomas represent the most common types of brain tumors. Among them, gliomas account for approximately 40-45% of all intracranial tumors and thus are the most common primary brain tumors. Depending on the specific type of cells, gliomas are classified into several subgroups, the most frequent being astrocytomas (accounts for 75% of all gliomas), oligodendroglial tumors, mixed gliomas (oligoastrocytomas), and ependymal tumors (3). Astrocytomas may be divided into two major groups. One group is more commonly seen with diffusely infiltrating properties. It includes astrocytoma, anaplastic astrocytoma, and

glioblastoma. The other group is less common with more circumscribed growth, comprising pilocytic astrocytoma, pleomorphic xanthoastrocytoma, and subependymal giant cell astrocytoma of tuberous sclerosis (3). Depending on histopathology, astrocytomas are divided into three grades of malignancy: World Health Organization (WHO) grade II diffuse astrocytoma, WHO grade III anaplastic astrocytoma, and WHO grade IV glioblastoma (4). The prognosis of brain tumors is among the worst of all tumors. Although patients with grade II or grade III astrocytomas may survive for 5 or 2-3 years respectively, most of grade IV glioblastoma patients survive substantially less than 2 years (1).

Genetic alterations play a key role in the development of astrocytomas. Inactivation of p53, a tumor suppressor encoded by the *TP53* gene, plays an important role in the development of at least one third of all adult astrocytoma (5, 6). The *PTEN* tumor suppressor gene at 10q23.3 is often deleted in astrocytoma, as loss of chromosome 10 is found to occur in 60% to 95% of glioblastoma multiforme (GBM) and to a lesser extent in anaplastic astrocytoma (7). Epidermal growth factor receptor (*EGFR*) is consistently reported to be amplified in approximately 40% of all GBM, resulting in over-expression of EGFR transcript and protein (8). Other genetic alterations include chromosomal losses mapping to 9p and 13q, all of which targets a critical cell cycle regulatory complex consisting of p16, cyclin-dependent kinase 4 (cdk4), cdk6, cyclin D1, and retinoblastoma (Rb) proteins. P16 controls cells from entering S phase by inhibiting the cdk4/cyclin D1 and/or cdk6/cyclin D1 complexes, preventing them from phosphorylating Rb, and so maintaining cells in the G1 phase of the cell cycle. The loss of chromosome 9p targets the *CDKN2A* locus, which encodes p16 protein, and the loss of 13q preferentially inactivates Rb function. They occur in approximately 50% (9p) or 30%-50% (13q) of high-grade astrocytomas (1).

3.1.2 Temozolomide and glioma chemotherapy

The standard treatments for glioma are surgery, radiation therapy and chemotherapy. Radiation therapy and/or chemotherapy are generally used as secondary or adjuvant treatments following surgery. However, radiation and chemotherapy may be used without surgery if the tumor is inoperable. Therapeutic alkylating agents, the mainstay of glioma chemotherapy, damage DNA by transferring alkyl-adducts to DNA bases. They include TMZ, nitrosourea-based alkylating agents, carmustine (bichloroethyl nitrosourea, or BCNU) and lomustine (chloroethylnitrosourea, or CCNU), streptozotocin, procarbazine and dacarbazine. Although BCNU and CCNU showed a modest effect as adjuvant therapy for GBM, their use has been supplanted by TMZ and the latter became the preferred and widely used alkylating agent in the treatment of glioma (9). In a landmark international trial, Stupp et al. reported that patients receiving radiotherapy plus concurrent TMZ followed by six cycles of adjuvant TMZ had significantly increased median and 2-year survival compared to those receiving radiotherapy alone after surgery (10). In a randomized phase II trial, TMZ also showed benefits over procarbazine in patients with recurrent glioblastoma, in terms of progression free survival and health-related quality-of-life (11). TMZ induces tumor cell cytotoxicity by adding a methyl group to DNA bases. There are three major types of base modifications. The major site of methylation is the N7 position of guanine (>70%) followed by the N3 position of adenine (9.2%) and the O^6 atom of guanine (5%) (12) **(Table 1.1)**. The N7 atom of guanine has the highest negative electrostatic potential of all the other atoms within DNA bases, which makes it the most vulnerable site to electrophilic attack by alkylators and N7-methylguanine (7MeG) constitutes the majority of TMZ-induced base lesions. 7MeG by itself does not possess any significant mutagenic or cytotoxic effects. However, over-

Table 1.1 TMZ-induced base lesions Chemical structures and corresponding frequencies of TMZ-induced DNA base lesions.	
	70%
	9.2%
	5%

expression of MPG, the mammalian repair enzyme that removes 7MeG lesions, sensitizes human breast cancer cells to TMZ by converting 7MeG into toxic repair intermediates (13, 14). While N3-methyladenine (3MeA) does not have major mutagenic effects, the cytotoxicity of 3MeA is well established in the literature (15). The cytotoxic effect of 3MeA derives from its ability to block replication and its potential to give rise to toxic repair intermediates following removal by MPG (16). If left un-repaired, O^6-methylgaune (O^6MeG) pairs with thymine during DNA replication and causes G→A transition mutations. It is the primary mutagenic lesion induced by most alkylation damage to the genome (17). The cytotoxicity of O^6MeG seems to be the primary contributor of cytotoxicity induced by TMZ. The mechanism has been shown to be related to abortive mismatch repair (MMR) (15). Two models have been proposed to explain the cytotoxicity induced by this lesion. The first suggests that MMR acts as a sensor of the O^6MeG:T

mispair and directly activates apoptotic signaling that involves ATR/ATRIP (18, 19). The second model proposes that cytotoxicity is due to futile cycling of the mismatch repair system at an O^6MeG:T base pair. The model proposes that, upon recognition of the O^6MeG:T mispair, MMR removes the newly incorporated thymine from the nascent strand. During repair synthesis, thymine is once again incorporated opposite the O^6MeG lesion, resulting in initiation of another round of repair by the MMR system. This recursive cycling of excision and synthesis is thought to produce DNA strand breaks that activate DNA damage signaling pathways, leading to cytotoxicity (20).

3.2   CHEMOTHERAPY RESISTANCE AND DNA REAPIR

3.2.1   Glioma chemotherapy resistance

Chemotherapy resistance of malignant glioma results from two major avenues, innate and acquired resistance, and resistance to alkylating agents is the major cause of treatment failure in patients with malignant brain tumors (21). Acquired resistance is normally related to the difficulties of delivering chemotherapeutics to tumor cells and reaching a homogenous cytotoxic concentration. Exposure of tumor cells to sub-lethal concentrations of drug increases the chances of acquired resistance (1). Despite the ability of TMZ to readily cross the blood brain barrier and to achieve an effective therapeutic concentration in the brain, the innate resistance of tumor cells remains the greatest obstacle to the successful treatment of glioma. Innate resistance is a result of specific cellular and genetic properties of tumor cells that efficiently repair and/or tolerate damage caused by chemotherapeutics. Deleterious genetic alterations in gliomas, for instance

loss of *p53* or *PTEN*, confer tumor cells the ability to circumvent cell cycle arrest and apoptosis and provide a mechanism of DNA damage tolerance. Primary GBM are resistant to apoptosis due to universal over-expression of BCL2L12, which blocks the activation of both caspase-3 and caspase-7 (22, 23). TMZ mainly induces three types of DNA base lesions, all of which are readily repaired by defensive repair mechanisms in cells, because those lesions are also continuously produced by endogenous insults present in cells (15). Two mechanisms are responsible for the repair of TMZ-induced base lesions. The 7MeG and 3MeA lesions are primarily repaired by the BER pathway and inhibition of the BER pathway through genetic means or via chemical inhibitors results in enhanced cytotoxicity of alkylating agents (24). The O^6MeG lesion is repaired by O^6-methylguanine-DNA methyltransferase (MGMT). MGMT conducts repair of the O^6MeG lesion through a suicide mechanism, which covalently transfers the methyl group on the O^6 atom of guanine to the conserved active-site cysteine of MGMT, restoring the guanine to normal and inactivating the MGMT protein (25). Although a proportion of gliomas have been found to lack the expression of MGMT due to hyper-methylation of the MGMT promoter and thus have diminished DNA repair activity, at least half of GBM express MGMT and the expression is associated with resistance to chemotherapy and poor prognosis (26). Therefore, it is important to either overcome resistance rendered by expression of MGMT or find an alternative that improves efficacy of chemotherapy in the presence of MGMT activity. In this study, I show how modulation of the BER pathway provides enhanced sensitization of glioma cells to TMZ and a detailed mechanism of the increased sensitization is demonstrated.

3.2.2 Base excision repair

BER is the predominant DNA damage repair mechanism for the repair of base lesions **(Figure 1.1)**. It not only protects normal cells from endogenous DNA damage derived from oxidation and alkylation, but also provides cancer cells with resistance to chemotherapy treatment. Under

Figure 1.1 The BER pathway
Simplified model of the short-patch base excision repair pathway.
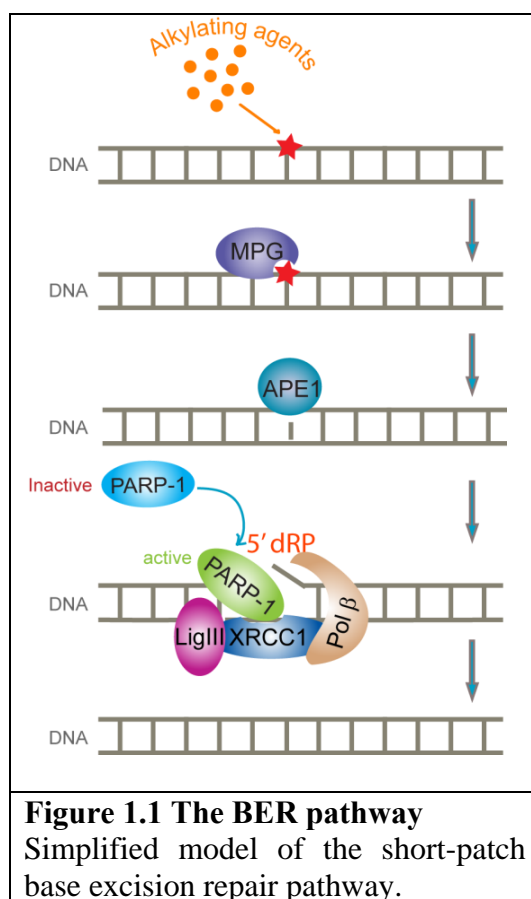
normal physiologic conditions, a functional BER pathway is essential to maintain genomic integrity as it has been estimated that 10^4 DNA bases are damaged per mammalian cell per day (27-29). The repair process is initiated with removal of damaged bases by a lesion-specific DNA glycosylase and completed by either a short-patch or long-patch BER mechanism. Following cleavage of the phosphodiester backbone immediately 5' to the abasic site (AP site) by

apurinic/apyrimidinic endonuclease 1 (APE1), via the so called short-patch BER pathway, Polß hydrolyzes the resulting 5'deoxyribose phosphate (5'dRP) moiety and inserts a single nucleotide. Alternatively, in the long-patch repair pathway, an overhang of 2 to 12 bases is produced by DNA polymerases (polymerase δ, ε, or ß) as a result of repair synthesis and strand displacement and the DNA overhang is excised by Flap endonuclease 1 (FEN1). It is currently thought that the majority of repair is carried out via the short-patch pathway (30). Following DNA strand incision, repair synthesis, and end tailoring if necessary, DNA Ligase I (LIGI) or a complex of DNA Ligase IIIα (LIGIIIα) and X-ray repair cross complementing protein 1 (XRCC1) complete the repair by sealing the nick in DNA (31).

3.2.3   Poly(ADP-ribosyl)ation and base excision repair

Poly(ADP-ribosyl)ation is a form of post translational modification of proteins that is mediated by poly(ADP-ribose) polymerases (PARP). PARP1 is the founding member of a large family of poly(ADP-ribose) polymerases with 17 members identified (32, 33). It is an abundant nuclear enzyme found in many eukaryotes, with the exception of yeast. It plays a primary role in the process of poly(ADP-ribosyl)ation, a post-translational modification that regulates a variety of cellular functions, including DNA repair, chromatin structure and transcription (32, 33). This highly conserved 113-kDa enzyme consists of three domains (34): an N-terminal 42-kDa DNA-binding domain, a 16-kDa automodification domain, and a 55-kDa C-terminal catalytic domain **(Figure 1.2)**.

The enzyme can be activated by a large spectrum of DNA damaging agents that directly or indirectly introduce DNA strand interruptions, including alkylating agents, reactive oxygen
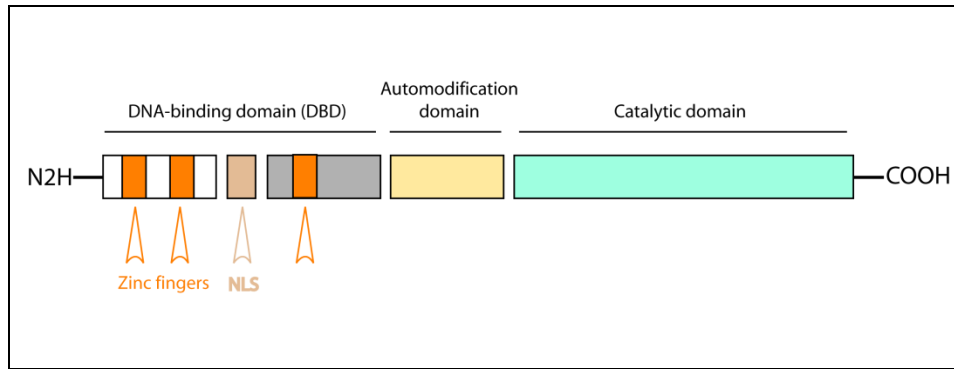
Figure 1.2 Schematic of the structure of human PARP1.
Three zinc fingers are present in the N-terminal DBD domain. They are responsible for DNA-binding, PARP1 enzymatic activity activation, and some protein-protein interactions. NLS, nuclear localization signal.

species, and ionizing radiation (33). The activated enzyme catalyzes the transfer of ADP-ribose units from donor NAD^+ molecules to many nuclear target proteins, including itself, as it is the primary acceptor of the modification (33). PARP1 has been suggested to play a role in necrosis. Previous research indicates that the PARP1-mediated ADP-ribosylation modification may alter the activity, function and cellular location of several cell death related factors. For example, it has been reported that PARP1 activation mediates translocation of apoptosis inducing factor (AIF) from the mitochondria to the nucleus, which results in large-scale DNA fragmentation and eventually cell death (35). Moreover, hyper-activation of PARP1, as a result of a high level of DNA damage, can lead to a rapid decrease in cellular NAD^+ levels and subsequent energy failure associated necrotic cell death (36, 37).

PARP1 was first suggested to play a role in BER by *in vitro* experimental evidence suggesting that PARP1 facilitates the repair of single-stranded DNA breaks (SSBs) in the presence of NAD^+ (38). Later, PARP1 KO mice and cells derived from those mice have been shown to be more sensitive to alkylation, radiation, and oxidative DNA damage compared to its wild type (WT) counterparts (39, 40), suggesting that PARP1 participates and contributes to the

13

repair of DNA base lesions. Physical interactions of PARP1 and BER proteins, including XRCC1 (41), Polß (39, 42), and LIGIIIα (43), and the functional interplay between PARP1 and XRCC1 (44) establish a role for PARP1 in BER.

3.2.4   Mechanism of base excision repair inhibition induced cytotoxicity

Efficacy of chemotherapy or radiation treatment is intimately dependent on DNA repair capacity (21). Robust repair of therapeutically induced DNA damage can provide significant resistance whereas tumor-specific defects in DNA repair or inhibition of specific DNA repair proteins can provide therapeutic advantage (45). In particular, inhibiting BER can be an effective means to improve response to TMZ, radiation, bleomycin and cisplatin, among other treatments (24, 46-52). Like most DNA repair pathways, BER is a multi-step mechanism comprised of greater than 20 proteins, depending on the initial base lesion (53). However, inhibiting each step in the BER pathway will have different outcomes. DNA glycosylase inhibition or loss blocks BER initiation, leading to the accumulation of both cytotoxic (54) and mutagenic base lesions (55), with the latter contributing to cellular dysfunction. In this regard, the preferred option is the inhibition of BER after repair initiation, promoting the accumulation of cytotoxic BER intermediates such as AP sites and SSBs by inhibiting AP site repair with MX, inhibiting the BER enzyme PARP1 or by loss or inhibition of Polß (45, 56, 57). We refer to inhibition of the intermediate steps in BER as the induction of "***BER failure***", since repair is initiated yet is unable to be completed.

Importantly, understanding the mechanisms that are responsible for the increase in cell death due to BER inhibition or BER failure is critical in tailoring treatment, as well as, designing rational adjuvant or combination treatments that may further increase overall response. For

example, inhibiting PARP1 has been shown to be effective in improving TMZ induced cell death (58). Inhibition of PARP1 results in the accumulation of replication-mediated DNA double-stranded breaks (DSBs) and the onset of apoptosis (59, 60). This detailed understanding of the mechanism of cell death induced by combining a DNA damaging agent (TMZ) and a PARP1 inhibitor suggests that PARP1 inhibition would be effective against many tumors but may be ineffective against tumors that are resistant to apoptosis (22). Further, cell death induced by PARP1 inhibition suggested a requirement for homologous recombination (HR) in the cellular response to the accumulated DSBs, prompting pre-clinical and clinical trials of PARP1 inhibitors in the treatment of HR defective tumors (45).

There are several BER proteins essential for the repair of TMZ-induced DNA lesions. Using a MEF cell model, we have shown that loss of Polß can significantly improve the cytotoxic effect of TMZ (51), suggesting that inhibition of Polß may improve response to TMZ in human tumor cells. TMZ is currently used in the treatment of glioblastoma (61) and it is therefore critical to evaluate the role of Polß in glioma cell response to TMZ treatment. No previous studies have investigated the role of Polß in the response of human glioma tumor cells to TMZ. Further, there is no mechanistic explanation for the increase in alkylation-induced cell death observed in cells that are deficient in Polß beyond the evidence that cell death in mouse cells is the result of accumulation of un-repaired BER intermediates (51, 57).

Acute alkylation damage has been suggested to induce cell death by multiple mechanisms, including necrosis (62), caspase-3 and caspase-9 activation and the onset of apoptosis (63), AIF translocation from the mitochondria to the nucleus (35, 64, 65), ADP-ribose induced activation of the Ca^{2+} channel TRPM2 or AMP-mediated inhibition of ATP transport (66-68). In most, if not all cases, cell death has been attributed to the direct action of either PAR

formed by PARP1 activation or PAR catabolites that accumulate after PAR degradation by the catabolic enzyme poly(ADP-ribose) glycohydrolase (PARG). Polß deficient mouse cells are hypersensitive to the cell killing effects of alkylating agents due to failure to repair the 5'dRP BER intermediate (69). However, the exact downstream signaling events and mechanism of cytotoxicity specifically induced by the un-repaired 5'dRP lesion remains unclear. Previous studies in mouse cells have not been conclusive. One report suggested that the absence of Polß led to damage-induced cell death via apoptosis (70) whereas a later study proposed a necrotic form of cell death for both wild-type and Polß deficient cells (71), similar to what has been proposed as a general mechanism of alkylation-induced cell death in mouse fibroblasts (62). However, this latter study required the use of apoptosis-deficient cells to observe necrotic cell death (62). None of these previous studies have identified a mechanism of cell death specific to Polß deficiency and BER failure or a failure to repair the cytotoxic BER intermediate 5'dRP.

The studies described herein were designed to specifically define the mechanism of cell death in human tumor cells resulting from failure to repair the BER intermediate 5'dRP due to 'inhibition of' or a 'deficiency in' Polß (***BER failure***). I have hypothesized that PARP1 functions in BER as both a complex coordinator and as a molecular repair sensor. As a BER molecular sensor, I suggest that PARP1 facilitates cell death in response to incomplete BER or BER failure. In support of this hypothesis, I show that a specific BER intermediate, a single-strand DNA strand break containing a 3'OH and 5'dRP, is an *in vivo* substrate in human cells that activates PARP1 in the context of BER and that elevated cytotoxicity observed in Polß deficient human cells is controlled by the activation of PARP1. Further, I provide clear evidence that following "BER failure", human cells die independent of receptor-interacting protein 1 (RIP1) activation or AIF translocation, thus ruling out PAR as the cell death signal that is

16

initiated upon BER failure. Further, I show that the observed cell death in Polß deficient cells is un-related to the accumulation of PAR catabolites such as ADP-ribose or AMP yet is dependent on NAD$^+$ metabolite bioavailability or the bioenergetic capacity of the cell.

This study provides mechanistic insight into why Polß deficiency leads to cell death, defines the mode of death and offers a mechanistic link between BER failure and energy metabolism - the novel finding that DNA damage-induced cytotoxicity mediated via BER inhibition is primarily dependent on cellular metabolite bioavailability. Finally, I offer a mechanistic justification for the elevated alkylation-induced cytotoxicity of Polß deficient cells, suggesting a linkage between DNA repair, cell survival and cellular bioenergetics.

3.2.5   Modulation of base excision repair in chemotherapy sensitization

TMZ is an oral chemotherapeutic agent approved for the treatment of anaplastic astrocytoma and newly diagnosed glioblastoma (72). It also showed clinical activity in metastatic melanoma and is under clinical evaluation for use in other cancers, including leukemia, lymphoma, aerodigestive tract, pancreatic and neuroendocrine tumors as well as cancers that have metastasized to the brain (73). TMZ causes cancer cell cytotoxicity by methylating genomic DNA, producing cytotoxic and/or mutagenic abnormal DNA bases (74). However, the ability of cancer cells to recognize and repair those DNA lesions confers chemotherapeutic resistance and limits therapeutic efficacy (21). The majority of TMZ-induced DNA lesions, including 7MeG and 3MeA, are repaired by the BER pathway (74), while the O^6MeG is directly removed by MGMT (75, 76). Although O^6MeG constitutes only a small proportion of the base lesions produced by TMZ, it is the most cytotoxic lesion and constitutes a significant level of TMZ-

induced cytotoxicity (73). Since O^6MeG-induced cytotoxicity is mediated through the MMR pathway, sensitivity to TMZ requires both low MGMT repair activity and functional MMR (73). At least half of glioblastoma multiforme (GBM) express MGMT and the expression is associated with resistance to chemotherapy and poor prognosis (26). Loss of the MMR protein MSH6, due to somatic mutations, has also been shown to be associated with glioblastoma recurrence post radiation and TMZ treatment (77). Therefore, it is important to either overcome resistance resulting from MGMT activity or find an alternative that improves efficacy of TMZ in the presence of MGMT activity. However, MGMT inhibitors (e.g., Patrin) have not shown clinical efficacy (73, 78). Pharmacological inhibition of the BER pathway, which repairs the 7MeG and 3MeA lesions induced by TMZ, has been shown to enhance TMZ-induced cytotoxicity independent of MGMT status (79).

The repair of TMZ-induced base damage by the BER pathway starts with the recognition and removal of the damaged bases by MPG, also known as alkyladenine DNA glycosylase (AAG) (76). The AP site produced following the action of MPG is then hydrolyzed by APE1 resulting in the incision of the damaged DNA strand and formation of a 3'OH group and a 5'dRP group in the repair gap (53). PARP1 together with poly(ADP-ribose) polymerase 2 (PARP2) and PARG recognizes the DNA strand interruption and facilitates the recruitment of subsequent BER proteins, including the BER scaffold protein XRCC1 and Polß (53). Polß subsequently hydrolyzes the 5'dRP moiety and inserts a single nucleotide, preparing the strand for ligation by a complex of DNA Ligase IIIα and XRCC1 to complete the repair process (69).

Enhanced sensitivity to alkylating agents has been observed by modulating the BER pathway in preclinical studies, suggesting BER modulation is an attractive option for chemotherapy potentiation (80). Currently, several BER proteins are under active investigation

as potential targets for chemotherapy sensitization, including APE1 (56), PARP1 (81), PARG (82) and Polß (51, 52, 83-85). MX is a small molecule that specifically inhibits BER (86). It is currently under a phase I clinical trial under the name of TRC102 (ClinicalTrials.gov Identifier: NCT00692159). MX inhibits repair of AP sites by binding and modifying the AP sites, rather than directly inhibiting the enzyme APE1. An AP site modified by MX is refractory to APE1, preventing it from processing by the ensuing steps of BER and is eventually cytotoxic (50). MX potentiates a wide range of DNA damaging agents that produce AP sites regardless of the status of MMR, MGMT, and p53 (56).

PARP1 is the primary enzyme in human cells that catalyzes the transfer of ADP-ribose units from NAD^+ to target proteins, including itself. Under normal physiologic conditions, PARP1 facilitates the repair of DNA base lesions by helping recruit BER proteins XRCC1 and Polß (87). Inhibition of PARP1 results in decreased repair of DNA base damage and increased sensitivity of cells to alkylating agents, which makes it an attractive and effective target for chemotherapy sensitization (88). Many PARP inhibitors have been developed and tested in several tumor types (89). They have been shown to enhance the cytotoxicity of TMZ against glioma (90-92), leukemia (93), lung (94, 95) and colon (95-97) carcinoma. It has been shown recently that a PARP inhibitor (ABT-888) + TMZ therapy has broad activity in multiple histologic types in subcutaneous and challenging orthotopic or metastatic models (98). PARG is the main enzyme responsible for degradation of PAR *in vivo* via endo- and exo-glycosidic cleavage. Although complete ablation of PARG activity leads to early embryonic lethality, embryonic stem cells derived from PARG null mouse (99) and cells from $PARG_{110}$ (one of three isoforms of PARG) deficient mice (100) have been shown to be sensitive to alkylating agents

and ionizing radiation. It has also been shown that inhibition of PARG activity sensitized malignant melanoma to TMZ in mouse models (82).

Over-expression of MPG has been reported to sensitize human breast cancer cells (52, 101), osteosarcoma cells (102), and ovarian cancer cells (49) to the chemotherapeutic agent TMZ. The increased sensitivity has been shown to be the result of increased repair initiation of the non-toxic 7MeG lesion (13), saturating the enzymatic activity of Polß resulting in accumulation of cytotoxic 5'dRP repair intermediates (51). Since BER inhibitors (e.g., AP site repair inhibition by MX, PARP or PARG inhibition) inhibit the repair steps following BER initiation, I hypothesized that MPG over-expression might further increase BER inhibitor-induced sensitization of glioma cells to the alkylating agent TMZ. In this study, I show that over-expression of MPG sensitizes glioma cells (LN428 and T98G) to MX, the PARP inhibitors PJ34 and ABT-888, or PARG inhibition (knockdown) following exposure to TMZ, suggesting that increased initiation of BER combined with inhibition of the ensuing repair steps provides enhanced sensitization of glioma cells to TMZ.

4.0 MATERIALS AND METHODS

4.1 MATERIALS

4.1.1 Chemicals and reagents

Alpha EMEM was from Mediatech. RPMI 1640 and DMEM were from Cambrex Bioscience Group and Biowhittaker, respectively. Fetal bovine serum (FBS), heat inactivated FBS, Pen/Strep/Ampho, glutamine and antibiotic/antimycotic were from InVitrogen. TMZ was obtained from the National Cancer Institute Developmental Therapeutics Program. A TMZ stock solution was prepared in dimethyl sulfoxide (DMSO) at 100 mM. Methyl methanesulfonate (MMS) was from Sigma-Aldrich. *N*-Methyl-*N*'-Nitro-*N*-Nitrosoguanidine (MNNG) was obtained from TCI America, dissolved in DMSO to a stock concentration of 10 mM, filtered through a 0.22 µm filter and stored at -20°C before use. Puromycin, Gentamicin and Neomycin were purchased from Clontech Laboratories, Irvine Scientific and InVitrogen, respectively. PJ34 and Z-VAD.fmk were purchased from Calbiochem. MX, Necrostatin-1, and 3-methyladenine (3-MA) were purchased from Sigma. BAPTA.AM was from InVitrogen. ß-nicotinamide mononucleotide (NMN) was from Sigma and Nicotinic Acid (NA) was obtained from Fisher. ABT-888 was kindly provided by Abbott Laboratories.

4.1.2 Plasmids, RNAi vectors and lentivirus preparation

Human MPG (WT) was expressed using the plasmid pRS1422, as described previously (52). The MPG expression plasmid (pRS1422) was then mutated at residue N169 using the Quickchange XL Site-Directed Mutagenesis Kit (Stratagene) to yield pIRES-Neo-MPG-N169D. The expression plasmid for FLAG-tagged WT human Polß was generated by PCR amplification of the human Polß cDNA using a FLAG-containing forward oligonucleotide and cloned into pENTR/D-TOPO as we described previously (52). pENTER/Flag-Polß(WT) was then mutated at residue K72 as described above to yield pENTER/Flag-Polß (K72A). Flag-Polß (WT) and Flag-Polß (K72A) was subsequently cloned into a Gateway-modifed pIRES-Puro vector by TOPO cloning, as we have described previously (52). The FIV-based lentiviral shRNA expression vector system specific for human Polß was as described previously (52) but was modified for copGFP expression (pSIF-H1-hPOLB1-copGFP). FIV-based lentiviral particles were generated by co-transfection of plasmid pCDF1-MCS1-EF1-copGFP (control) or pSIF-H1-hPOLB1-copGFP (Polß shRNA) together with pFIV-34N and pVSV-G into 293-FT cells (103) using FuGene 6 Transfection Reagent (Roche). HIV-based lentiviral particles for co-expression of PARG shRNA and TurboGFP was prepared by transfection of four plasmids (the control plasmid pLK0.1-Puro-tGFP or the human PARG-specific shRNA plasmid pLK0.1-Puro-PARGshRNA4, plus pMD2.g(VSVG), pRSV-REV and pMDLg/pRRE) into 293-FT cells (104, 105) using FuGene 6 transfection reagent (Roche Diagnostic Corp, Indianapolis, IN). Culture media from transfected cells was collected 48 hours after transfection to isolate the viral particles, passed through 0.45 µm filters, used immediately or stored at -80°C in single-use aliquots.

4.2   METHODS

4.2.1   Cell culture and cell line development

The cell line LN428 is an established glioblastoma-derived cell line with mutations in *TP53*, deletions in *p14^{ARF}* and *p16* and is WT for *PTEN* (106, 107). LN428 cells were kindly provided by Ian Pollack (University of Pittsburgh) and were cultured in Alpha EMEM supplemented with 10% heat inactivated FBS, glutamine, antibiotic/antimycotic and Gentamycin. MDA-MB-231 cells and derivatives were described previously (52). Human MPG (WT), human MPG (N169D), Flag Polß (WT) and Flag Polß (K72A) expressing cell lines were developed by transfection using FuGene 6 Transfection Reagent (Roche) according to the manufacturer's protocol. Transfected cell lines were cultured in G418 and/or Puromycin for 2 weeks and individual clones stably expressing human MPG or Polß were selected. It was recently suggested that p14^{ARF} deficiency results in proteosome-mediated degradation of Polß (108). Although LN428 cells are deficient in p14^{ARF} (107), we note that the expression levels of Polß are stable. Transduction of LN428 cells with control lentivirus (GFP expression only) or human Polß or PARG specific shRNA lentivirus was completed as follows: Briefly, 6.0×10^4 cells were seeded into 6-well plates and incubated for 24-30 hours at 10% CO_2 at 37°C. Cells were transduced for 18 hours with virus at 32°C and cultured for 72 hours at 37°C before isolation of the GFP-expressing population by fluorescence-activated cell sorting (FACS) using the University of Pittsburgh Cancer Institute Flow Cytometry Facility. Cells were then cultured to expand the population and analyzed for expression of the target gene by qRT-PCR and/or immunoblot. MGMT over-expression LN428 cell lines were developed by plasmid transfection. Briefly, 1.5×10^5 cells were seeded into 60mm dishes and incubated for 24-30 hours (5% CO_2 and at 37°C). The human

23

MGMT expression plasmid (pIRES-Puro-hMGMT) was transfected using FuGene 6 Transfection Reagent (Roche, Indianapolis, IN) according to the manufacturer's instructions. Stable cell lines were selected in puromycin (0.5 μg/ml) for 2 weeks, individual clones (stably expressing human MGMT) were expanded and 30 μg of nuclear extract was analyzed by immunoblot analysis for the expression of human MGMT protein. All the cell lines developed and used in this study are described in **APPENDIX A**.

4.2.2   Quantitative RT-PCR analysis

Expression of PARG and Polß mRNA was measured by quantitative RT-PCR using an Applied Biosystems StepOnePlus system. Briefly, 80,000 cells were lysed and reverse transcribed using the Applied Biosystems Taqman® Gene Expression Cells-to-CT™ Kit. Each sample was analyzed in triplicate and the results are averages of all three analyses. Analysis of mRNA expression was conducted as per the manufacturer instructions ($\Delta\Delta C_T$ method) using Applied Biosystems TaqMan® Gene Expression Assays (human Polß: Hs00160263_m1; human PARG: Hs00608254_m1) and normalized to the expression of human ß-actin (part #4333762T).

4.2.3   Cell extract preparation and immunoblot

Nuclear extracts were prepared and protein concentration was determined as we described previously (51). Briefly, cells were washed with cold PBS, pelleted, and lysed using NucBuster™ Protein Extraction Kit (Novagen). Protein concentration was determined using Bio-

Rad Protein Assay (Bio-Rad). Twenty microgram of protein was loaded on a pre-cast 4-20% NuPAGE Tris-Glycine gel (InVitrogen). For whole cell extracts used in PAR formation assays, 3×10^6 cells were seeded into a 100 mm cell culture dish 24 hours before drug treatment. Cells were either treated with TMZ only or pre-exposed to a PARP inhibitor (PJ34 or DR2313) followed by PARP inhibitor plus TMZ treatment. After treatment, cells were washed twice with cold PBS, collected and lysed with 400 μL of 2X Laemmli buffer (2% SDS, 20% Glycerol, 62.5 mM Tris-HCl pH6.8, 0.01% Bromophenol Blue). Samples were boiled for 8 min and extract from approximately 1.5×10^5 cells were loaded each lane of a 4-12% pre-cast NuPAGE Tris-Glycine gel (InVitrogen) for immunoblot analysis.

The following primary antibodies were used in immunoblot analyses: anti-human MPG (Mab; clone 506-3D) (52); anti-Pol ß (Mab clone 61; Thermo Fisher Scientific); anti-APE1 (EMD Biosciences); anti-PCNA (Santa Cruz); anti-Flag (M2 Mab; Sigma-Aldrich); anti-poly(ADP-ribse) (PAR) (Clone 10H, kindly provided by M. Ziegler); anti-poly(ADP-ribose) polymerase-1 (PARP1) (BD Pharmingen) and anti-human HMGB1 (R&D Systems); anti-MGMT (Novus, Littleton, CO).

4.2.4 Cell cytotoxicity assay

Short-term MTS cell survival assay: TMZ or TMZ + MX induced cytotoxicity was determined by an MTS assay, a modified MTT assay as described previously (51). For PJ34, DR2313, Z-VAD.fmk, 3-MA, necrostatin-1, BAPTA-AM, and MX, cells were pre-exposed to the inhibitor for 30 minutes (PJ34, DR2313, necrostatin-1, BAPTA-AM, and MX) or one hour (Z-VAD.fmk and 3-MA) and were then treated with TMZ in the presence of the inhibitor for 48 hours. For NA

and NMN, cells were pre-exposed to each for 24 hours (concentrations as indicated in the legend) and were then treated with TMZ (1.0 mM) in the presence of NA or NMN for 48 hours. The impact on cell growth and survival was determined by an MTS assay, as described previously (51). Results were calculated from the average of three or four separate experiments and are reported as the percentage of treated cells relative to the cells without treatment (% Control).

Long-term cell survival assay: Cells were seeded into 6-well plate with cell growth media without neomycin and/or puromycin 24 hours before exposure to PJ34 (4 μM), ABT-888 (10 μM) or DMSO as control. 30 minutes later, cells were treated with TMZ alone, TMZ plus PJ34 (2 μM) or TMZ plus ABT-888 (5 μM) for 6 hours. Cells were washed with PBS, trypsinized, resuspended and counted before being re-seeded into three 100 mm cell culture dishes at 8000 cells (for LN428 cell lines) or 3000 cells (for T98G cell lines) each in cell growth media without neomycin and/or puromycin. Cells were incubated with or without 2 μM PJ34 or 5 μM ABT-888 for 10 days and the cells were counted. Results were calculated from three independent experiments and reported as percentage relative to the control treatment (% Control).

4.2.5 PAR assay

Cells (1.5×10^6) where seeded in 100mm dishes 24 hours before treatment. Media was then removed and replaced with fresh media or media supplemented with PJ34 (2 μM). After 30 minutes, cells were lysed immediately (0 time point) or media was replaced with TMZ for the times indicated in the figure legends. Extracts were prepared by washing the cells with cold PBS and preparing cell extract with 400 μl of 2X Laemmli Buffer. 20 μl of the cell extract was

analyzed by immunoblot with a 4000-fold dilution of an anti-PAR primary antibody (Clone 10H) followed by a 5000-fold dilution of the horseradish peroxidase (HRP)-conjugated secondary goat anti-mouse Ab.

4.2.6 HMGB1 release assay

Cells were pre-treated with media alone or with PARP inhibitor (PJ34) for 30 min before co-treatment with PJ34 (2 μM) and TMZ (1.5 mM) for 12 hours. Cell culture media was then collected and passed through 0.45 μM filters. 100 μL of immoblized Heparin (Thermo Fisher Scientific) slurry and 1 mL of media were mixed and rotated at 4°C for 2 hours before centrifugation at 8,000g to pull-down HMGB1 bound to immobilized Heparin (109). Pellets were boiled with 100 μL of 2X Laemmli buffer and supernatants were used for immunoblot analysis after brief centrifugation.

4.2.7 Subcellular fractionation and analysis of AIF translocation

Cells were seeded into 100 mm cell culture dishes at 3×10^6 cells / dish. 24 hours later, cells were treated with TMZ (1.5 mM) for different periods of time before washing with cold PBS and subjecting to cell fractionation, essentially as described (110). Briefly, following treatment and washing, cells were collected by scraping using a rubber scraper. Cells were pelleted (400g, 5 min at 4°C). The cell pellet was resuspended in 1 ml of cold homogenization buffer (0.25 M sucrose, 10 mM HEPES pH 7.4, 1 mM EGTA) and the cell suspension was homogenized in a 2 ml Wheaton Dounce Homogenizer on ice. The homogenate was centrifuged at 1,000g for 15

27

minutes at 4°C to obtain the nuclear pellet, and the supernatant was then centrifuged at 10,000g

for 15 minutes at 4°C to pellet mitochondria.

4.2.8   Molecular beacon MPG activity assay

Oligonucleotides used for the molecular beacon assay were purchased from Integrated DNA

Technologies (Coralville, USA): FD-Con, 6-FAM-dGCACTATTGAATTGACACGCCATGTC

GATCAATTCAATAGTGC-Dabcyl, where 6-FAM is carboxyfluorescein and Dabcyl is 4-(4'-

dimethylaminophenylazo) benzoic acid; FD-MPG1, 6-FAM-dGCACT**X**TTGAATTGACACGC

CATGTCGATCAATTCAATAGTGC-Dabcyl, where **X** is 1, N^6-ethenoadenine (εA).

These oligonucleotides were designed to form a stem-loop structure with 13 nucleotides situated

in the loop and 15 base pairs in the stem. To ensure that the beacons correctly adapted their stem-

loop structure, they were heated at 95°C for 3 min and slowly cooled down to room temperature.

Once the hairpin is formed, no measurable fluorescence was detected (not shown) and the

hairpin is stable at 37°C for greater than 120 minutes. However, when heated to 95°C, the

hairpin unfolds, resulting in maximum fluorescence intensity (not shown). Nuclear protein

extracts were first prepared as described above then dialyzed twice in the following buffer for 90

min: 50 mM Hepes pH7.5, 100 mM KCl, 0.5 mM EDTA, 20% Glycerol and 1 mM DTT.

Reactions were performed using 2 µg of dialyzed protein extract and the FD-Con or FD-MPG1

beacon (40 nM) in the following buffer: 25 mM HEPES-KOH pH7.8, 150 mM KCl, 0.5 mM

EDTA, 1% Glycerol, 0.5 mM DTT. Fluorescence was measured using a StepOnePlus real-time

PCR system and expressed as arbitrary units (AU).

5.0   RESULTS

5.1   MECHANISM OF ALKYLATION SENSITIVITY MEDIATED BY INHIBITION OF BASE EXCISION REPAIR

5.1.1   Base excision repair imbalance in human glioma cells increases cell sensitivity to alkylation damage

BER is a finely tuned process that requires balanced expression of several proteins to avoid accumulation of mutagenic or cytotoxic repair intermediates (53). Further, multiple cellular factors control the response to the accumulation of base lesions or repair intermediates, resulting in varying outcomes when BER is inhibited or defective. For example, deficiency of the BER enzyme Mpg in the mouse provides resistance to alkylation-induced retinal degeneration and bone-marrow toxicity whereas -Mpg deficient mouse embryonic stem (ES) cells are sensitive to alkylation damage (111-113). Deficiency or inhibition of PARP1, another critical BER enzyme, has diverse outcomes, providing resistance to ischemia and stroke-induced neuronal cell death (114, 115) but sensitization to chemotherapy (45, 46). To understand how alterations in BER enzyme activity in human tumor cells leads to DNA damage-induced cell sensitivity, I developed human glioma (LN428) cell lines with a functional deficiency in Polß by increasing expression of MPG and depleting the cell of Polß by stable expression of shRNA (**Figure 2.1A**).
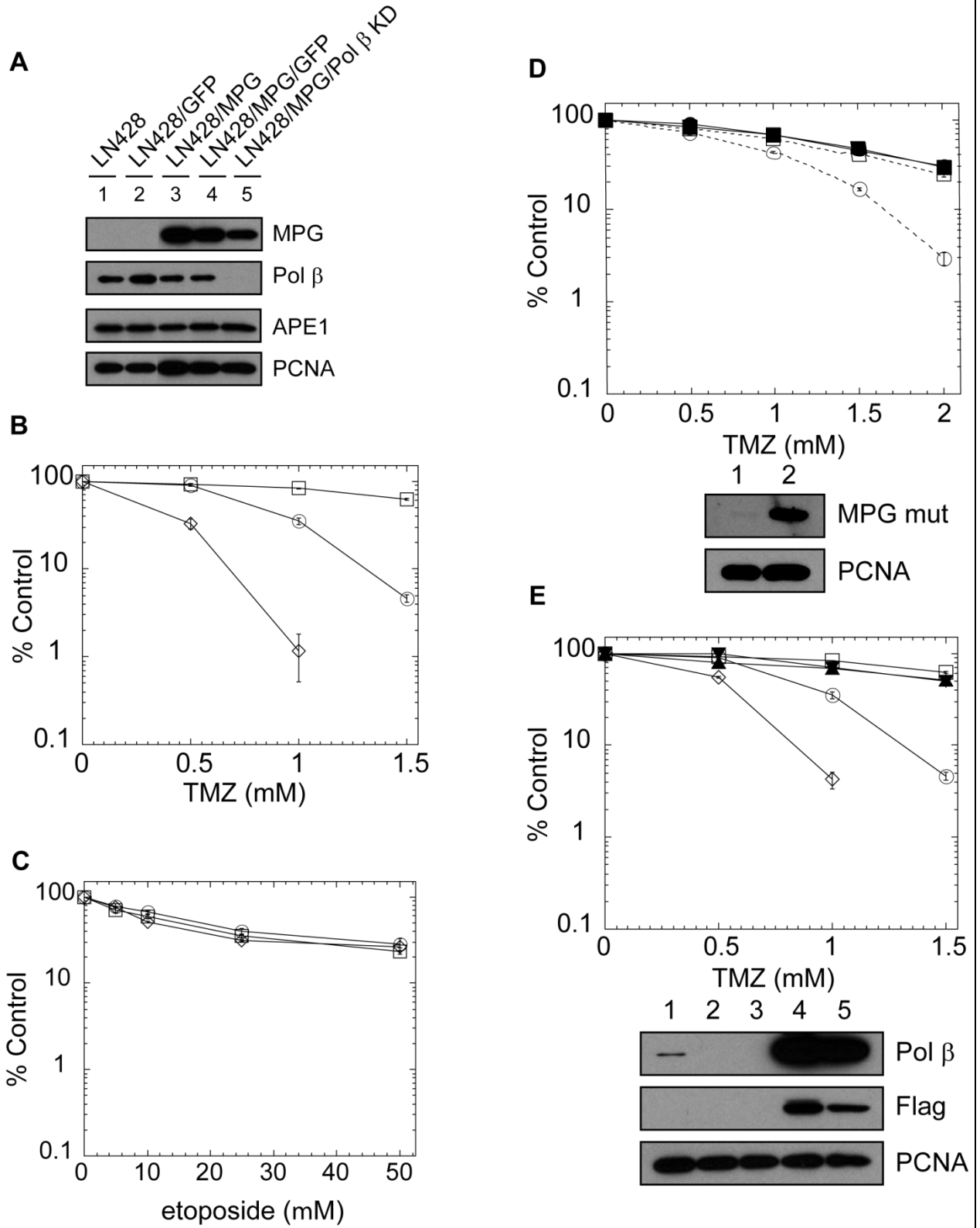
Figure 2.1

Figure 2.1 Alkylation sensitivity mediated by a deficiency in Pol ß-mediated DNA repair.
(A) Characterization of glioma cell lines. Expression level of BER proteins including MPG, Polß and APE1 are shown for LN428 glioma cells (LN428), LN428 cells transduced by GFP expressing lentivirus (LN428/GFP), LN428 cells transfected with plasmid pIRES.neo.MPG to over-express MPG (LN428/MPG), MPG over-expressing glioma cells expressing GFP (LN428/MPG/GFP) or co-expressing GFP and Polß shRNA (LN428/MPG/Polß-KD). PCNA was used as a loading control.
(B) Cell sensitivity to TMZ. Cells were cultured in 96-well plates for 24 hours prior to exposure to TMZ. After treatment (48 hrs), viable cells were determined using a modified MTT assay. Plots show the % viable cells as compared to untreated (control) cells. Means are calculated from quadruplicate values in each experiment. Results indicate the mean ± S.E. of three independent experiments. [LN428, open square; LN428/MPG, open circle; LN428/MPG/Polß-KD, open diamond]
(C) Cell sensitivity to etoposide (ETO) exposure for 48 hours. Viable cells were measured as in (B). [LN428, open square; LN428/MPG, open circle; LN428/MPG/Polß-KD, open diamond]
(D) (*Upper panel*) Cellular cytotoxicity due to TMZ treatment in LN428 cells over-expressing either WT or a glycosylase null mutant of MPG (N169D) following 48 hour exposure to TMZ. Viable cells were measured as in (B). [LN428, open square; LN428/MPG, open circle; LN428/MPG-mut, filled circle] (*Lower panel*) Western blots showing over-expression of mutant N169D-MPG (lane 2) as compared to LN428 cells transfected with the vehicle control (lane 1).
(E) (*Upper panel*) Cellular cytotoxicity due to TMZ treatment in LN428/MPG/Polß-KD cells complemented with Flag tagged WT Polß (clone 2 and 6) following 48 hour exposure to TMZ. Viable cells were measured as in (B). [LN428, open square; LN428/MPG, o]en circle; LN428/MPG/Polß-KD, open diamond; LN428/MPG/Flag-Polß-WT, filled triangle; LN428/ MPG/Polß-KD /Flag-Polß-WT, filled triangle] (*Lower panel*) Over-expression of Flag tagged Polß (WT) in the LN428/MPG/Polß-KD cell line. An immunoblot from two representative clones (clone 2 and 6; lanes 4 and 5) are shown, compared to LN428/MPG cells (lane 1), LN428/MPG/Polß-KD cells (lane 2) and LN428/MPG/Polß-KD cells transfected with the vehicle control (lane 3).
This figure is reproduced with permission from Supplemental Figure S1 of my recent publication in *Mol Cancer Res* (85).

As we have reported, human cells with elevated expression of MPG are sensitive to alkylation damage due to a deficiency in Polß (52). This DNA damage sensitive phenotype is enhanced by Polß knockdown (Polß-KD) (**Figure 2.1A, B**). This is in-line with a previous report by Dr. Sobol that Polß deficiency-induced sensitization of mouse fibroblasts to alkylating agents requires the expression of -Mpg (116). Cells were depleted of Polß by lentiviral-mediated expression of Polß specific shRNA, as we have described previously (52). Expression of Polß protein was not detectable by immunoblot (**Figure 2.1A, lane 5**) whereas Polß mRNA was reduced to 30% of the control, as determined by qRT-PCR (**not shown**).

I find that over-expression of MPG alone and in combination with Polß knockdown (**Figure 2.1A**) sensitizes human glioma cells to DNA damage induced by the alkylating agents TMZ (**Figure 2.1B**), MMS and MNNG (**Figure 2.8A**) but not damage induced by a control DNA-damaging agent (an agent that causes DNA damage not repaired by BER), the topoisomerase II inhibitor etoposide (**Figure 2.1C**). Also as a control, I show that *(i)* this hypersensitive phenotype was not observed in cells expressing inactive MPG (**Figure 2.1D**) and *(ii)* over-expression of Polß eliminated the hypersensitive phenotype (**Figure 2.1E**), demonstrating that the increased alkylation sensitivity in the LN428/MPG and LN428/MPG/Polß-KD cells is due to a deficiency in Polß-mediated DNA repair. These cells are therefore functionally deficient in Polß and they were utilized to determine the mechanism that regulates the enhanced DNA damage-induced cell death resulting from Polß deficiency.

5.1.2 Hyperactivation of PARP due to Polß deficiency and failure to repair the BER intermediates 5'dRP

The DNA binding and signaling molecules PARP1 and PARP2 have each been implicated in BER (53). PARP1 facilitates BER complex formation and it has been postulated that local, strand-break induced activation of PARP1 and the resultant synthesis of PAR mediates recruitment of the BER proteins XRCC1 and Polß to stimulate DNA repair (87). I therefore have hypothesized that in cells that fail to complete BER (e.g., when 5'dRP lesions are not repaired; herein referred to as '**BER Failure**'), PARP1 is hyper-activated and functions as a DNA damage signaling protein that triggers cell death. To determine whether PARP is activated by the BER intermediate (5'dRP) *in vivo*, I exposed the control (LN428) and corresponding BER defective cells (Polß deficient LN428/MPG and LN428/MPG/Polß-KD cells) to TMZ for up to 90 minutes. Whole cell extracts were probed by immunoblot for PAR accumulation following TMZ exposure (**Figure 2.2A**). The level of PAR accumulation was shown to correlate with the extent of the BER defect. PARP activation was elevated in the LN428/MPG cells (an intermediate level of sensitivity), with the highest level of PAR observed 30 minutes following exposure to TMZ whereas essentially no PARP activation was observed in the LN428 cells (**Figure 2.2A**). In the more sensitive cell line (LN428/MPG/Polß-KD), PARP activation was more robust and rapid as compared to that of the LN428/MPG cell line (**Figure 2.2A**), as PAR reached its highest level at 15 minutes after exposure to TMZ. To ensure that these findings are not unique to this cell line, we characterized a second cell line in which Polß was depleted, the breast cancer cell line MDA-MB-231. Comparable results were also observed in a Polß defective breast cancer cell line where elevated TMZ-induced PARP activation is restricted to the cells with Polß deficiency (85). Conversely, exposure to etoposide resulted in a low level of PARP activation at all time points
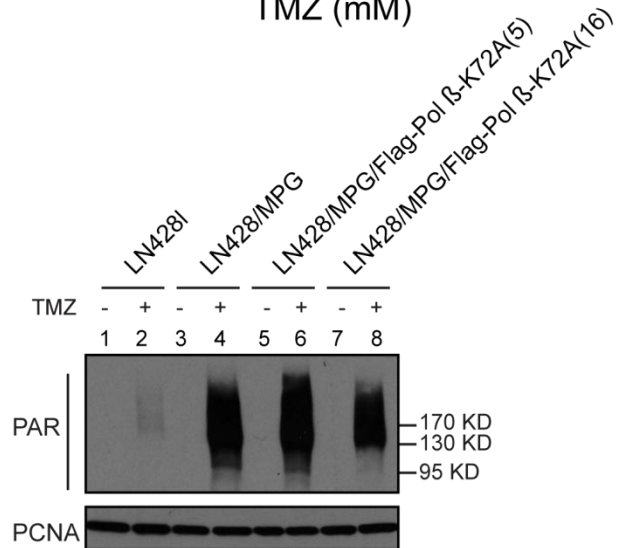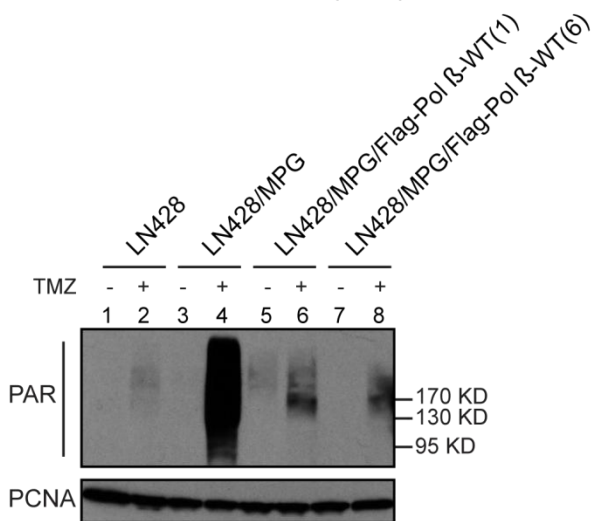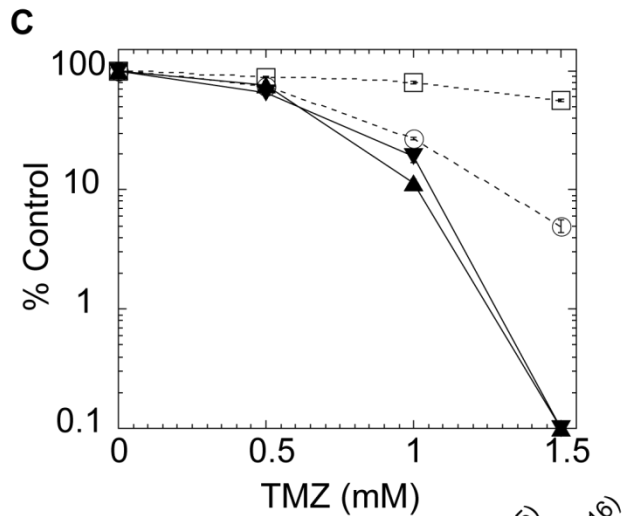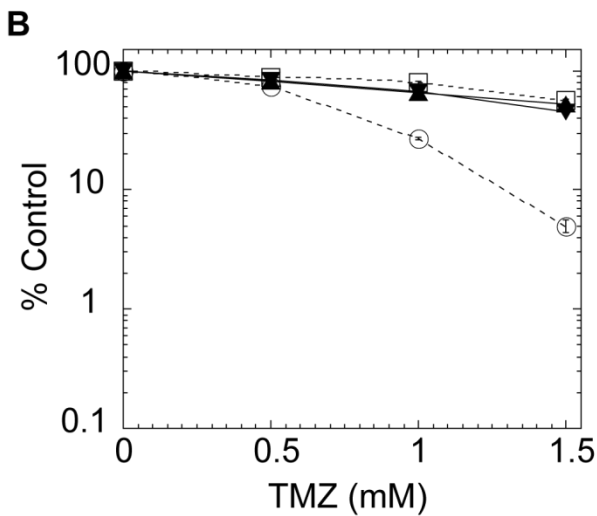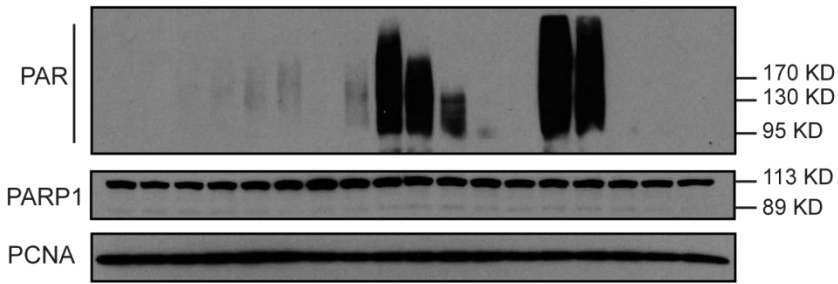
Figure 2.2 PARP activation due to BER failure
(A) Immunoblot of PAR to determine activation of PARP after exposure to TMZ (1.5mM) for the time indicated. PARP1 and PCNA protein expression levels are also shown.
(B) (*Upper panel*) TMZ induced cytotoxicity in LN428, LN428/MPG and two clones of

LN428/MPG cells complemented with Flag-Polß-WT, measured as in Figure 2.1A. [LN428, open square; LN428/MPG, open circle; LN428/MPG/Flag-Polß-WT, clones 1 and 6, filled triangle] (*Lower panel*) Immunoblot of PAR to determine activation of PARP1 after exposure to TMZ (1.5mM) for the time indicated. PCNA is shown as a loading control.

(C) (*Upper panel*) TMZ induced cytotoxicity in LN428, LN428/MPG and two clones of LN428/MPG cells complemented with Flag-Polß-K72A, measured as in Figure 2.1A. [LN428, open square; LN428/MPG, open circle; LN428/MPG/Flag-Polß-K72A, clones 5 and 16, filled triangle] (*Lower panel*) Immunoblot of PAR to determine activation of PARP1 after exposure to TMZ (1.5mM) for the time indicated. PCNA is shown as a loading control.

This figure is reproduced with permission from Figure 1 of my recent publication in *Mol Cancer Res* (85).

for all three cell lines LN428, LN428/MPG, and LN428/MPG/Polß-KD (**Figure 2.8B**). Thus, PARP activation is elevated in BER defective (Polß deficient) cells following alkylation damage.

Since the combination of alkylating agent treatment and Polß deficiency triggers PARP activation, I next validated the significance and specificity of this finding by re-expression of Polß in the LN428/MPG and LN428/MPG/Polß-KD cells. I find that the BER deficient phenotype (increased cellular sensitivity to alkylating agents) observed in both the LN428/MPG and LN428/MPG/ Polß-KD cells was reversed by complementation (expression) of FLAG-Polß (WT) (**Figure 2.1E & 2.2B,** *upper panel*) but not the 5'dRP lyase deficient (K72A) mutant of Polß (**Figure 2.2C,** *upper panel*). Similarly, I find that complementation with FLAG-Polß (WT) but not with the Polß 5'dRP lyase mutant eliminated the TMZ-induced activation of PARP observed in BER defective cells (**Figure 2.2B & C;** *lower panel*). These data therefore suggests that the Polß specific BER intermediate (5'dRP lesion) triggers rapid and robust PARP1 activation *in vivo*, triggering the onset of cytotoxicity.

5.1.3 PARP activation is required for the alkylation sensitivity of Polß deficiency cells

The correlation between PARP activation and alkylation sensitivity prompted us to determine if inhibition of PARP reverses the cellular hypersensitivity of Polß deficient human tumor cells. I inhibited activation of PARP by pre- and co-treatment with the PARP1/PARP2 inhibitors PJ34 or DR2313. While the level of PARP activation in the control cells (LN428) in the presence or absence of the PARP inhibitor PJ34 or TMZ remains very low (**Figure 2.3A**; lanes 1, 2 & 5, 6), pre-treatment with PJ34 for 30 minutes followed by co-treatment with PJ34 and TMZ for an additional 30 minutes significantly reduced the level of PARP activation in the Polß deficient cells (LN428/MPG) (**Figure 2.3A**; lanes 3,4 & 7,8). I next assayed if PARP inhibition can rescue the alkylation-sensitive phenotype of LN428/MPG cells, as determined by an MTS assay 48 hours after TMZ exposure. Most importantly, I find that PARP inhibition by either PJ34 or DR2313 treatment converted the LN428/MPG cells from a sensitive phenotype to a resistant phenotype (**Figure 2.3B, C**). Rescue by PARP inhibition was also observed in Polß deficient MDA-MB-231 cells (85). These studies support our hypothesis that PARP activation is required for the alkylation sensitive phenotype of Polß deficient cells.

5.1.4 Base excision repair intermediates trigger cell death via energy depletion in the absence of PAR or PAR-catabolite mediated signaling

The mechanism of cell death due to failure to repair the Polß substrate (a 5'dRP containing DNA repair gap) is not known. I therefore systematically evaluated the involvement of caspase-dependent, autophagy-dependent and caspase-independent cell death mechanisms in control cells

Figure 2.3
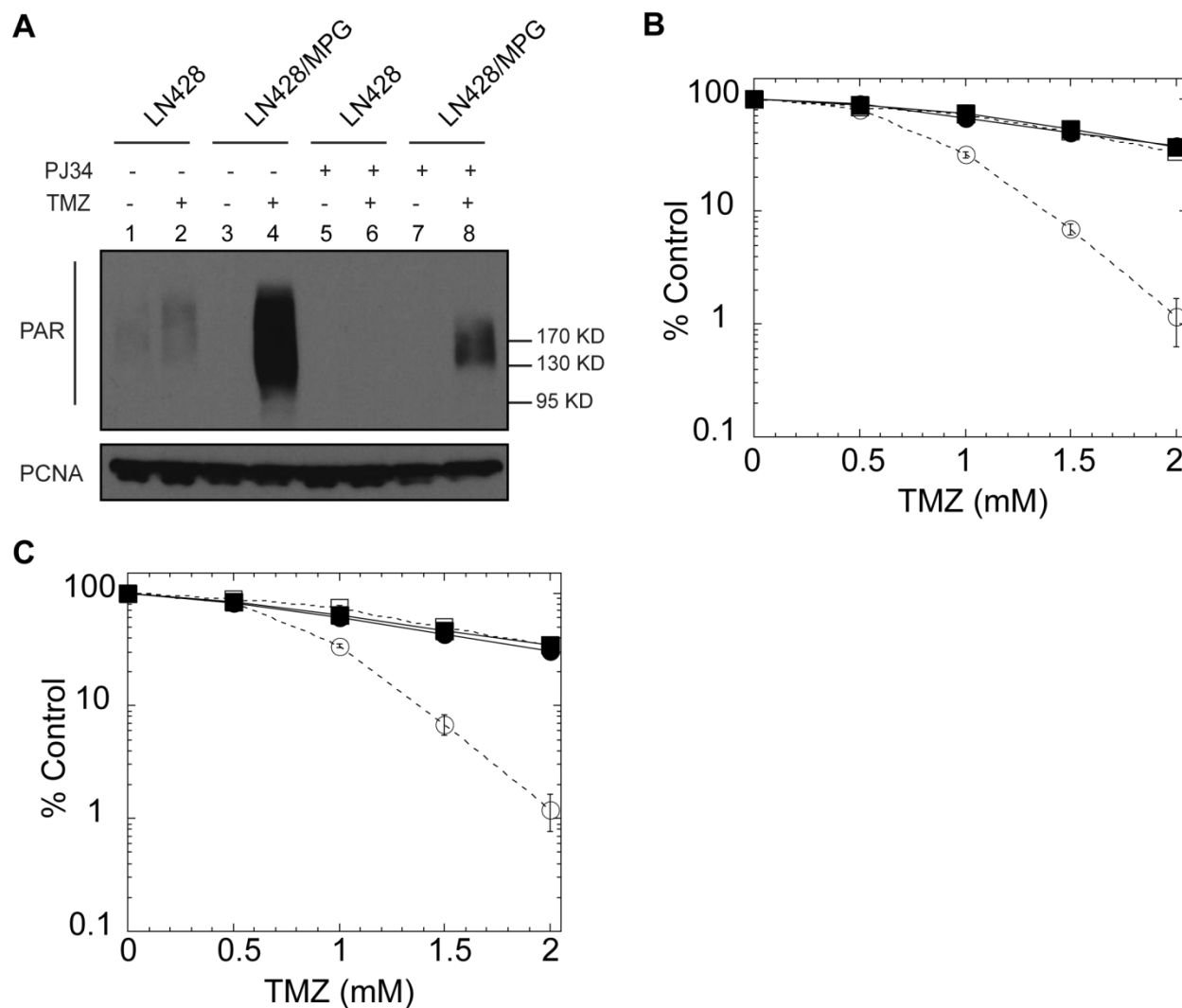
Figure 2.3 PARP activation mediates cellular hypersensitivity in BER defective cells
(A) TMZ induced PARP activation in LN428 and LN428/MPG cells in the presence or absence of the PARP1/PARP2 inhibitor PJ34. Cells were pre-treated with PJ34 (4 μM) or vehicle control for 30 min before exposure to TMZ (1.5 mM) plus PJ34 (2 μM) for another 30 min. PCNA was used as a loading control.
(B) TMZ induced cytotoxicity (LN428 and LN428/MPG cell lines) in the presence (solid lines) or absence (dashed lines) of the PARP1/PARP2 inhibitor PJ34. Viable cells were measured 48 hours after exposure as in Figure 2.1B. [LN428, open and filled square; LN428/MPG, open and filled circle]
(C) TMZ induced cytotoxicity (LN428 and LN428/MPG cell lines) in the presence (solid lines) or absence (dashed lines) of the PARP1/PARP2 inhibitor DR2313. Viable cells were measured 48 hours after exposure as in Figure 2.1B. [LN428, open and filed square; LN428/MPG, open and filled circle]
This figure is reproduced with permission from Figure 2 and Supplemental Figure S3.A of my recent publication in *Mol Cancer Res* (85).

as compared to the corresponding Polß deficient cells following TMZ treatment. The increased

sensitivity of the Polß deficient LN428/MPG cells, as compared to the control (LN428) cells was

unaffected by the presence of the pan caspase inhibitor Z-VAD.fmk (**Figure 2.4A**). Whereas

etoposide exposure of both the control and repair defective cells resulted in elevated caspase-3

and -9 activation, little or no activation of caspase-3 or -9 was observed following 24 hours of

TMZ exposure in all of the cell lines tested (85). Importantly, there is no difference in caspase

activation when comparing the control cells (LN428) to the BER defective cells (LN428/MPG)

(85). Both of these experiments therefore rule out a caspase-dependent response due to BER

failure, in-line with our previous report (52). Although it has been demonstrated that an

autophagic-response contributes to TMZ-induced cell death in some cells (117), TMZ

hypersensitivity of Polß deficient cells is not affected by the autophagy inhibitor 3-MA (**Figure

2.4B**). In support of this observation, we did not observe increased LC3 puncta in BER defective

cells following TMZ exposure (52). Finally, one of the hallmarks of caspase-independent cell

death is secretion of HMGB1 into the extracellular space (118, 119). A significant level of

HMGB1 was secreted into the culture media following exposure of BER defective cells

(LN428/MPG) to TMZ as compared to that of the control LN428 cells (**Figure 2.4C**). HMGB1

release was mediated through PARP activation, likely due to PARP1 modification (119), as

PARP inhibition greatly reduced the release of HMGB1 in BER defective cells (**Figure 2.4C**). It

is unclear how or if HMGB1 release due to failed BER is related to the recently reported role of

HMGB1 in BER (120). In all, these data eliminate a role for either an autophagic or caspase-

dependent mechanism of cell death due to BER failure and together with the data presented

above, provide support for a PARP1-activation induced mechanism of caspase-independent cell

death upon alkylating-agent exposure of Polß deficient cells.
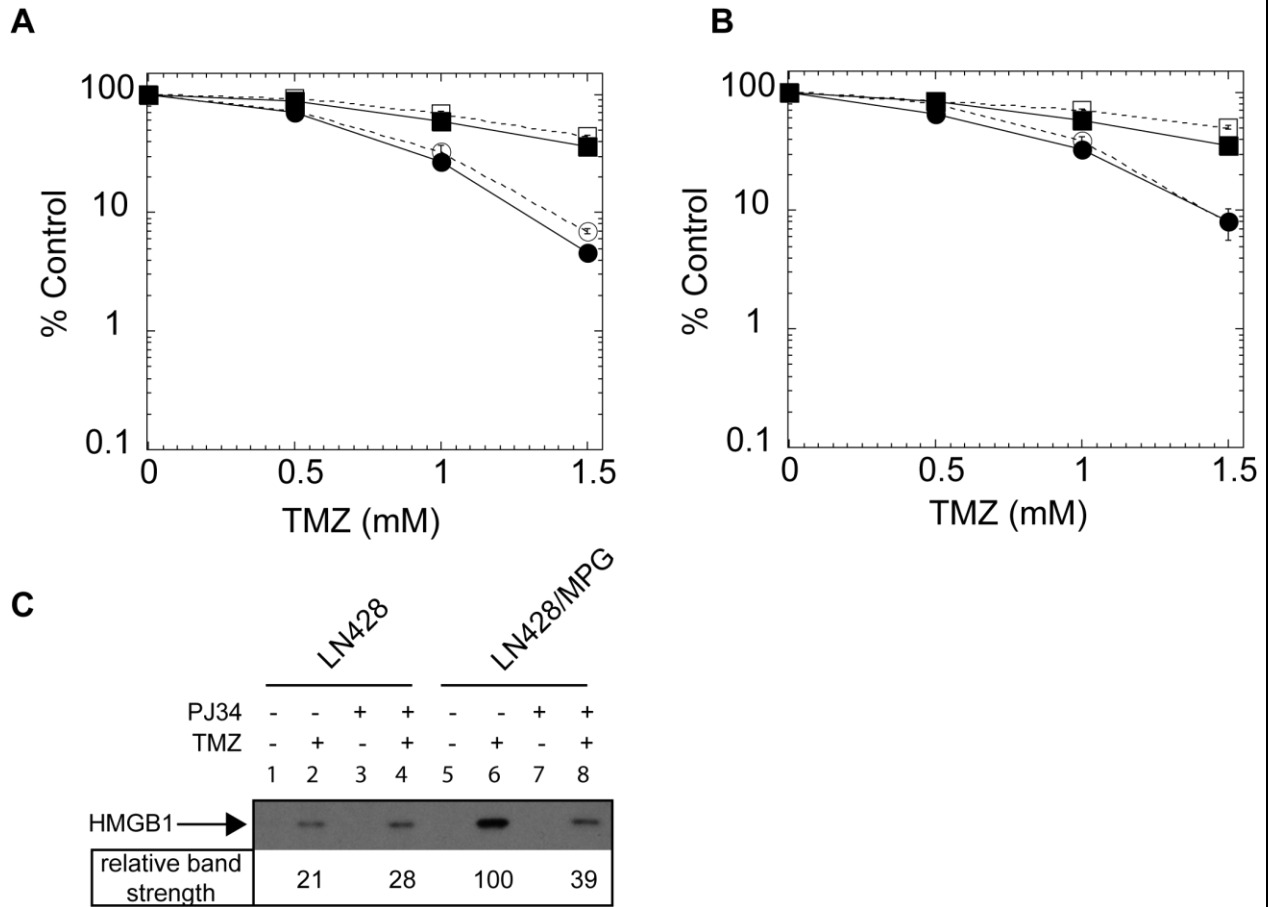
Figure 2.4 Alkylating agents induce PARP-dependent, caspase-independent cell death in Pol ß deficient LN428 cells.

(A) TMZ-induced cytotoxicity in LN428 and LN428/MPG cells with or without pan caspase inhibitor Z-VAD.fmk (50 µM). Viable cells were measured 48 hours after exposure as in Figure 2.1B. [LN428, open square; LN428 + Z-VAD.fmk, filled square; LN428/MPG, open circle; LN428/MPG + Z-VAD.fmk, filled circle]

(B) TMZ-induced cytotoxicity in LN428 and LN428/MPG cells with or without pre-treatment with the autophagy inhibitor 3-MA (4 mM). Viable cells were measured 48 hours after exposure as in Figure 2.1B. [LN428, open square; LN428 + 3-MA, filled square; LN428/MPG, open circle; LN428/MPG + 3-MA, filled circle]

(C) HMGB1 released into the cell culture media, as demonstrated by immunoblot. LN428 and LN428/MPG cells were pre-treated with PJ34 (4 µM) or vehicle control for 30 min and then exposed to TMZ (1.5 mM) with or without PJ34 (2 µM) for 12 hours. HMGB1 was then captured using immobilized heparin and analyzed by immunoblot, as described in the Experimental Procedures section.

This figure is reproduced with permission from Figure 3.D and Supplemental Figure S4.A & Figure S4.C of my recent publication in *Mol Cancer Res* (85).

A number of different mechanisms have been attributed to PARP1-induced cell death. In one of these, cell death results from direct PAR signaling to the mitochondria where PAR mediates translocation of AIF from the mitochondria to the nucleus to induce caspase-independent cell death (35, 64, 65) via a mechanism that requires RIP1 activation (121) (**Figure 2.5A**). RIP1 is a serine-threonine kinase that functions as a key regulator of the cell death signaling pathways initiated by multiple insults (122). Further, RIP1 has been suggested to be involved in DNA damage-induced, p53-independent, caspase-independent cell death (123, 124). In addition, RIP1 controls PAR-mediated signaling to facilitate PARP1-induced AIF translocation from the mitochondria to the nucleus and the resulting cell death (121). RIP1 can be inhibited by necrostatins, small molecule inhibitors shown to inhibit cell death (125, 126). Therefore, I investigated the role of RIP1 in the PARP-mediated cell death by inhibiting RIP1 with necrostatin-1 (126) and evaluating the impact of RIP1 inhibition on DNA damage-induced cell survival in both control and Polß deficient cells. However, inhibition of RIP1 did not prevent cell death in either the parental or Polß deficient cells (**Figure 2.5B**), suggesting but not proving that AIF translocation may not be related to the observed cell death.

We therefore next evaluated the sub-cellular localization of AIF in control and Polß deficient cells following exposure to the alkylating agents MMS or TMZ as compared to vehicle (media) by sub-cellular fractionation and immunoblot analysis (**Figure 2.5C**) or by immunofluorescent staining and confocal microscopy (85). In-line with the RIP1 inhibition data above, alkylating agent treatment of Polß deficient cells did not alter the sub-cellular localization of AIF as shown by subcellular fractionation analysis (**Figure 2.5C**) and immunofluorescent microscopy evaluation (85). All the detectable AIF was localized to the mitochondria in both cell
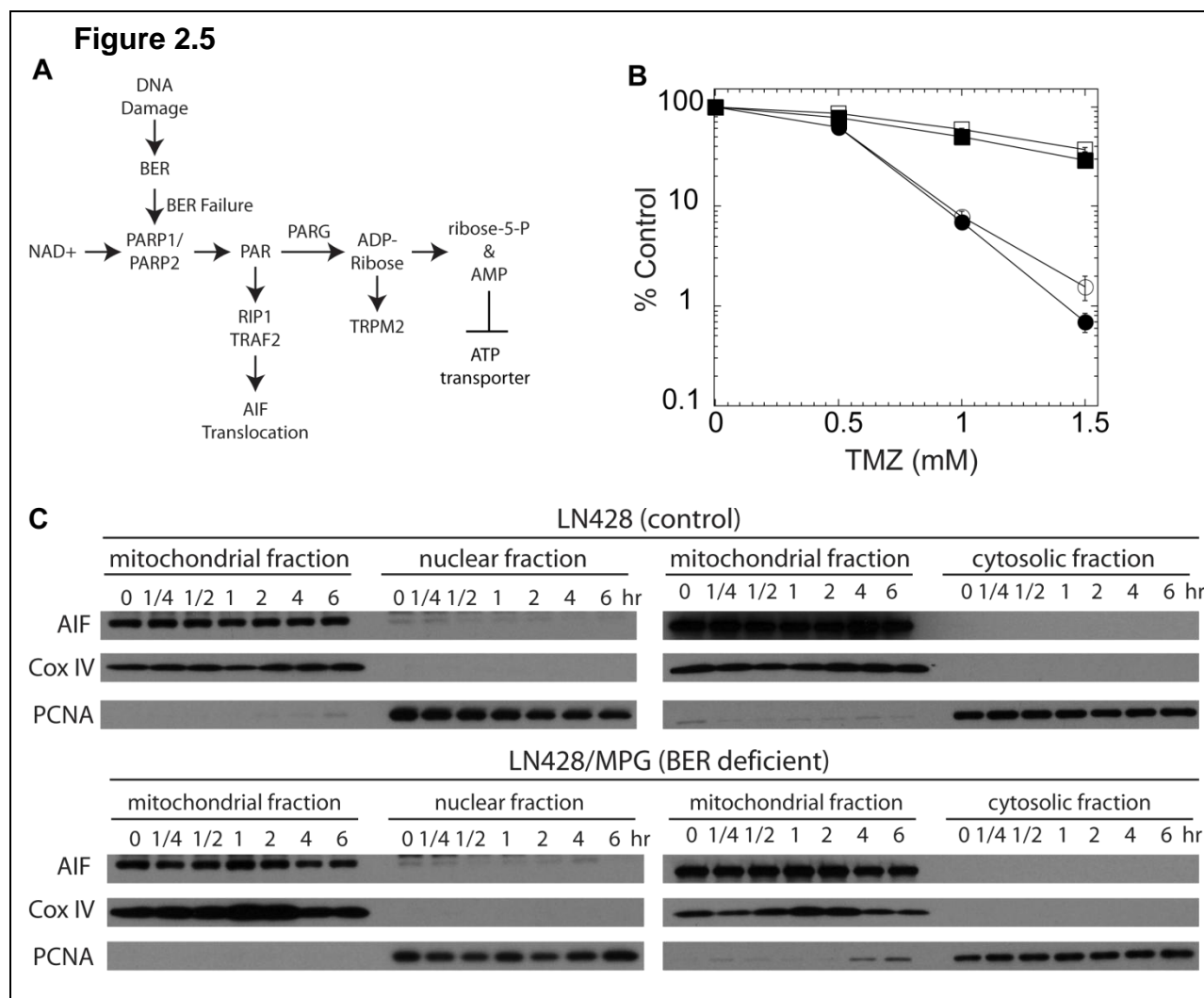
Figure 2.5

Figure 2.5 Absence of PAR mediated cell death following BER failure
(A) Model depicting the nexus of BER, the synthesis of PAR and the generation of PAR catabolites.
(B) Inhibition of RIP1 by necrostatin-1 does not protect cells from TMZ-induced cytotoxicity. Cells were pre-treated with necrostatin-1 or vehicle control (DMSO) for 30 minutes and were then exposed to TMZ in the presence or absence of necrostatin-1 (100 μM) for 48 hours. Viable cells were measured 48 hours after exposure as in Figure 2.1B. [LN428, open square; LN428 + necrostatin-1, filled square; LN428/MPG, open circle; LN428/MPG + necrostatin-1, filled circle]
(C) Absence of mitochondria to nucleus translocation of AIF due to BER failure as determined by subcellular fractionation and immunoblot analysis. Cells were treated with 1.5 mM TMZ for the times indicated in the figure and subjected to subcellular fractionation and immunoblot analysis. COX IV and PCNA were used as controls to show no cross contamination between mitochondrial and nuclear fractions. COX IV and PCNA were also used as loading controls to show that equal amount of mitochondrial or nuclear samples were loaded.
This figure is reproduced with permission from Figure 3.A and Supplemental Figure S5 & S6 of my recent publication in *Mol Cancer Res* (85).

lines regardless of agent or time of exposure (up to 12 hours), thus ruling out PAR as a cell death signal upon BER failure.

In the absence of a PAR-mediated cell death process (AIF translocation), it is possible that cell death is initiated via the rapid breakdown of PAR (see **Figure 2.2A**) by the degradative enzyme PARG and the accumulation of the PAR catabolites ADP-ribose, ribose-5-phosphate and/or AMP (**Figure 2.5A**) (127). ADP-ribose acts as a second messenger to activate the cation channel TRPM2 to trigger Ca^{2+} influx, resulting in cell death (66, 67) or inhibit ABC transporters (128) whereas elevated AMP can block ATP transport, leading to ATP depletion and cell death (68). To investigate the possibility that PAR catabolites contribute to PARP-mediated cell death in Polß deficient cells, I first blocked Ca^{2+} influx with BAPTA-AM, shown recently by Boothman and colleagues to abrogate PARP1-activation induced cell death (129, 130). Unlike that observed following DNA damage from reactive oxygen species or oxidative stress, BAPTA-AM did not prevent the elevated damage-induced cell death in Polß deficient cells (**Figure 2.6A**). However, as there may be multiple mechanisms of PAR-catabolite-induced cell death, I next knocked-down expression of PARG by stable-transduction of both cell lines with a lentivirus expressing shRNA specific to PARG. Expression of PARG mRNA is reduced to 35% as compared to the GFP-control cells when determined by qRT-PCR (**not shown**). Importantly, I found no evidence for PAR degrading activity in the cells with stable depletion of PARG (**Figure 2.6B**). PARG knockdown cells (LN428/MPG/PARG-KD) do not accumulate spontaneous PAR (lane 1) yet when exposed to an alkylating agent, BER deficient PARG-KD cells accumulate significant levels of PAR with no evidence for PAR degradation (**Figure 2.6B, lanes 2-4**). This is in contrast to the presence of PARG, when the PAR molecule is degraded within 60-90 minutes (**Figure 2.2, lanes 7-12**). These data demonstrate that these PARG-KD
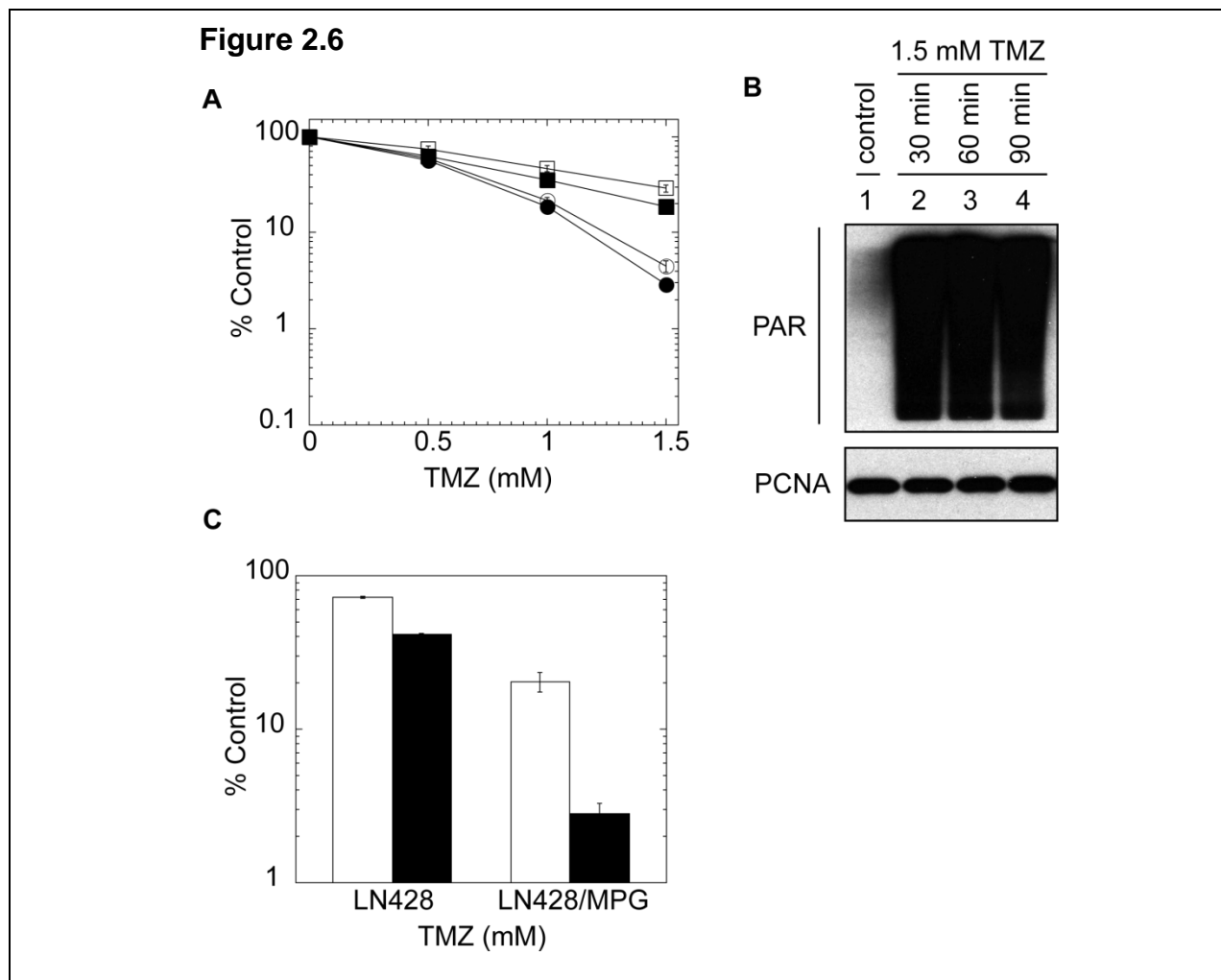
Figure 2.6

Figure 2.6 Absence of PAR-catabolite mediated cell death following BER failure
(A) Inhibition of Ca^{2+} influx by BAPTA.AM does not protect cells from TMZ-induced cytotoxicity. Cells were pre-treated with BAPTA.AM or vehicle control (DMSO) for 30 minutes and were then exposed to TMZ in the presence or absence of BAPTA.AM (5 mM) for 48 hours. Viable cells were determined as in Figure 2.1B. Results were reported as the mean of three independent experiments ± S.E.M. [LN428, open square; LN428 + BAPTA.AM, filled square; LN428/MPG, open circle; LN428/MPG + BAPTA.AM, filled circle]
(B) PARG KD prevented degradation of DNA damage-induced PAR. Immunoblot of PAR to determine the degradation of PAR in LN428/MPG cells following treatment with 1.5 mM TMZ. PCNA protein expression level was shown as a loading control.
(C) Preventing generation of PAR catabolites from degradation of PAR via PARG KD does not protect cells from TMZ-induced cytotoxicity. LN428 and LN428/MPG cells with (black solid bars) or without (white empty bars) PARG KD were exposed to TMZ (1 mM) or vehicle control (DMSO) for 48 hours. Viable cells were determined as in Figure 2.1B and reported as percentage relative to vehicle control treated cells (% Control). Error bars represent S.E.M from three independent experiments.
This figure is reproduced with permission from Figure 3.C and Supplemental Figure S7 of my recent publication in *Mol Cancer Res* (85).

cells do not degrade PAR and hence do not accumulate PAR-catabolites, providing an opportunity to determine if PAR catabolites contribute to cell death in these cells. As shown in **Figure 2.6C**, PARG-KD did not rescue or reverse the enhanced damage-induced cell death phenotype of Polß deficient (LN428/MPG) cells. In fact, PARG-KD cells (black bars) were more sensitive to the cell killing effect of the alkylating agent TMZ as compared to the PARG expressing cells (open bars)(**Figure 2.6C**). The inability of necrostatins to abrogate the response and the lack of PAR-mediated AIF translocation strongly suggests that PAR is not acting as a signaling molecule to induce cell death, as has been suggested (131, 132). Further, the inability of BAPTA-AM and most importantly, PARG-KD, to reverse the alkylation-sensitive phenotype of Polß deficient cells also suggests that the observed cell death is un-related to the accumulation of PAR catabolites such as ADP-ribose or AMP (**Figure 2.5A**).

An alternate process of cell death due to PARP1 activation was originally proposed by Berger to involve energy (NAD^+ and ATP) depletion (133, 134), in support of an earlier observation by Jacobson and colleagues demonstrating a decrease in NAD^+ concurrent with an increase in PAR synthesis (135). We therefore measured NAD^+ and ATP levels in the control (LN428) and Polß deficient (LN428/MPG and LN428/MPG/Polß KD) cells before and after exposure to MMS or TMZ. In line with the cytotoxicity and PARP1 activation results described above, exposure of Polß deficient cells to MMS or TMZ led to a rapid and drastic depletion of both NAD^+ and ATP whereas the NAD^+ and ATP levels in the control cells were not affected (85). We next measured the impact of alkylation damage on the corresponding cells depleted of PARG (PARG-KD). If PAR catabolites trigger cell death, we would expect that NAD^+ and ATP loss would be attenuated in PARG-KD cells. However, exposure of Polß deficient PARG-KD cells to TMZ led to enhanced depletion of both NAD^+ and ATP (85). The absence of PAR or
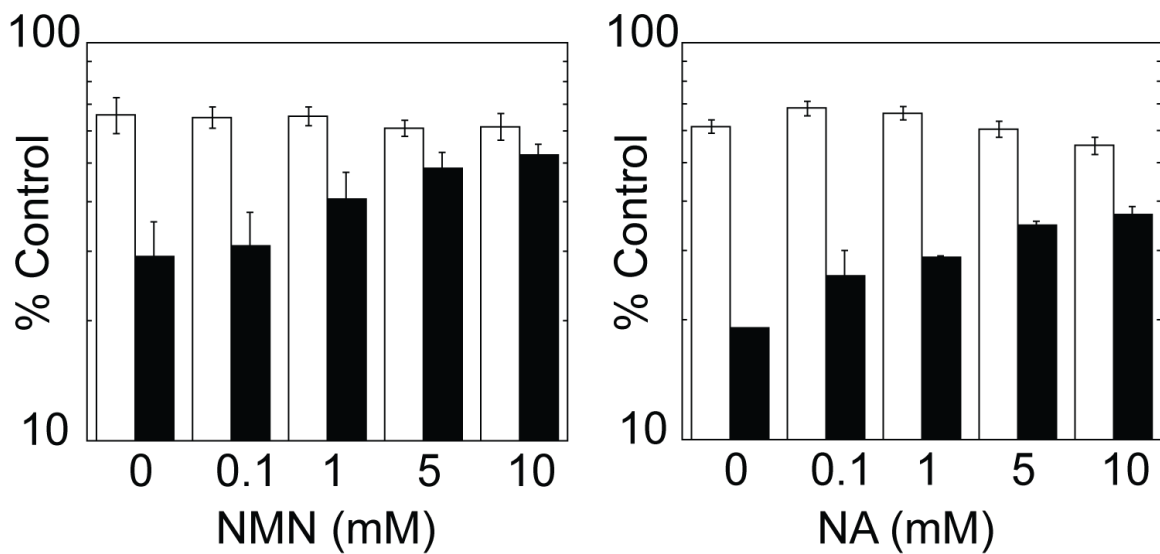
Figure 2.7 BER failure induced cell death depends on NAD^{+} availability
Bioenergetic metabolites rescue Polß deficient cells from DNA damage-induced cell death. LN428 and LN428/MPG cells were pre-treated with NMN, NA or vehicle control (media) for 24 hours and were then exposed to TMZ (1 mM) in the presence or absence of NMN or NA for 48 hours. Viable cells were measured as in Figure 2.1B. Results were reported as percentage relative to vehicle control treated cells (% Control) from three independent experiments $\pm$ S.E.M. This figure is reproduced with permission from Figure 4.C of my recent publication in *Mol Cancer Res* (85).

PAR-catabolite mediated cell death together with the specific loss of NAD^{+} and ATP even when the formation of PAR-catabolites are prevented (85), suggests that the BER failure response is linked to the cellular bioenergetic capacity of the cell.

For this paradigm to hold, I hypothesized that the availability of bioenergetic metabolites would impact the survival of Polß deficient cells exposed to an alkylating agent. In-line with this hypothesis, I find that supplementation of the cells with either NMN (136) or NA reversed the DNA damage-induced phenotype, rendering the Polß deficient cells (black bars) completely (NMN) or 90% (NA) resistant to the cell killing effects of the alkylating agent, as compared to

Figure 2.8

A
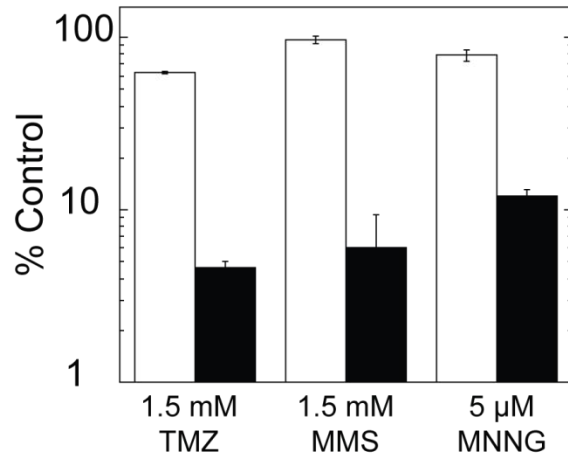
B
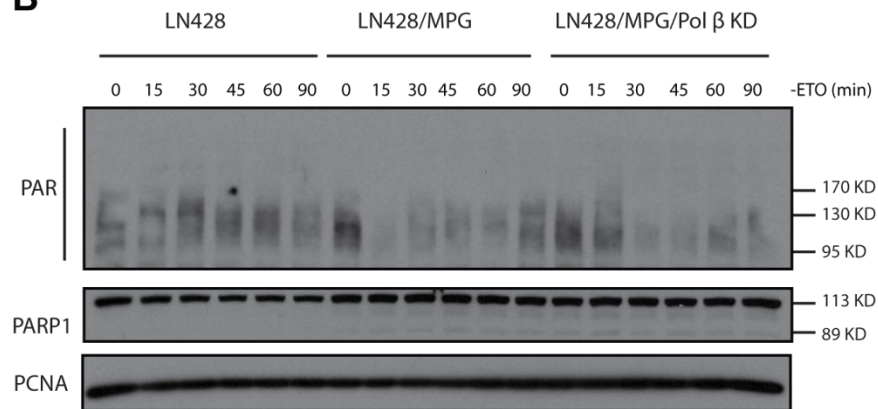
Figure 2.8 Glioma cell response to MMS, MNNG and etoposide
(A) Hypersensitivity of Polß deficient cells to TMZ, MMS and MNNG. Control cells (LN428, open bars) were resistant to alkylating agents, while the Polß deficient cells (LN428/MPG, black bars) were significantly more sensitive. Cells were exposed to 1500μM TMZ, 1500μM MMS or 5μM MNNG for 48 hrs. Cell survival was determined by an MTS assay, while percent survival was normalized to untreated control cells, as in Figure 2.1B. Results are reported as the mean from three independent experiments and error bars represent S.E.M.
(B) Immunoblot of PAR to determine activation of PARP1 after exposure of LN428, LN428/MPG and LN428/MPG/Polß KD cells to 50μM etoposide (ETO) for the time indicated. This figure is reproduced with permission from Supplemental Figure 2A & D of my recent publication in *Mol Cancer Res* (85).

the BER proficient cells (open bars) (**Figure 2.7**). Conversely, we anticipated that the hypersensitive phenotype of Polß deficient cells would be exacerbated by a reduction in the cellular level of NAD$^+$ and related bioenergetic metabolites. We therefore evaluated the impact of transient NAD$^+$ depletion on the observed "**BER Failure**" response by pre-treating cells with FK-866, a highly specific non-competitive small molecule inhibitor of nicotinamide phosphoribosyltransferase (NAMPT), a critical enzyme in the NAD$^+$ biosynthetic salvage pathway that catalyzes the synthesis of NMN (137). Most importantly, the sensitivity of control cells to alkylation damage was not altered by FK-866 treatment. However, the BER deficient cells are 9-fold more sensitive to MMS following a non-toxic (10 nM) treatment with FK-866, as compared to the untreated cells (85) even though PAR synthesis after the combined FK-866 + MMS treatment is attenuated (85). These results support our overall hypothesis that the BER failure phenotype of Polß deficient cells is mediated by BER intermediate (5'dRP) induced PARP1 activation and induction of caspase-independent cell death that is uniquely dependent on the availability of bioenergetic metabolites such as NMN and NAD$^+$.

5.2   N-METHYLPURINE DNA GLYCOSYLASE ENHANCES BER INHIBITION-INDUCED POTENTIATION OF GLIOMA CELLS TO TEMOZOLOMIDE

5.2.1   MX-induced potentiation of TMZ is enhanced by over-expression of N-methylpurine DNA glycosylase

To test our hypothesis that increased repair initiation by MPG will further sensitize glioma cells exposed to BER inhibitors, I stably over-expressed WT MPG in the glioma cell line LN428.

Over-expression of MPG was confirmed at the protein and mRNA levels using both immunoblot (**Figure 3.1A**) and qRT-PCR analyses, respectively (**Figure 3.1B**), with an approximate 40-fold increase of mRNA.

To confirm increased glycosylase activity in the MPG over-expressing cells (LN428/MPG), I developed a fluorescent MPG activity assay using a modified form of molecular beacons, similar to those previously reported for oxidative damage (138). These molecular beacon repair substrates are stem-loop structures formed by single-stranded DNA with a fluorophore (6-FAM) and a quencher (Dabcyl) on either end of the oligonucleotide. A 1,N^6-ethenoadenine (εA), a substrate of MPG, was positioned in the stem region of the beacon at base #5 from the 5'end and is used to probe for MPG activity. The same beacon structure with a normal adenine was used as the control substrate. Following removal of the 1,N^6-ethenoadenine lesion by MPG and subsequent DNA strand excision by APE1 5' to the AP site, at 37°C the 5-base long oligonucleotide containing the fluorophore 6-FAM separates from the quencher containing oligonucleotide and fluorescence signal can be detected at a wavelength of 517 nm as a measure of MPG activity (**Figure 3.1C**). Results of these experiments showed that the LN428/MPG cell line (**Figure 3.1D**, filled circle) had higher MPG activity as compared to the LN428 cell line (**Figure 3.1D**, filled rectangle). Cell extracts from both cell lines showed no activity when tested with the control substrate (**Figure 3.1D**, empty symbols), excluding the possibility that 6-FAM fluorescence signal results from non-specific cleavage of the molecular beacon.

Using a short-term cell survival assay (48-hour MTS assay), I next assayed the potentiation of TMZ by MX in the LN428 cells with or without MPG over-expression. MX sensitized both cell lines to TMZ. In the LN428 cells, MX induced a 1.5-fold increase in

Figure 3.1
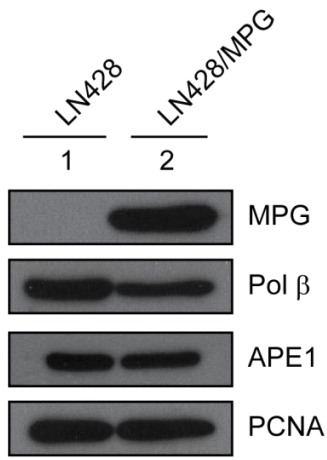
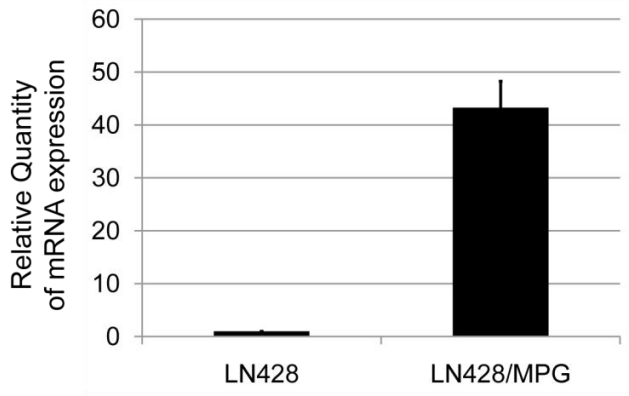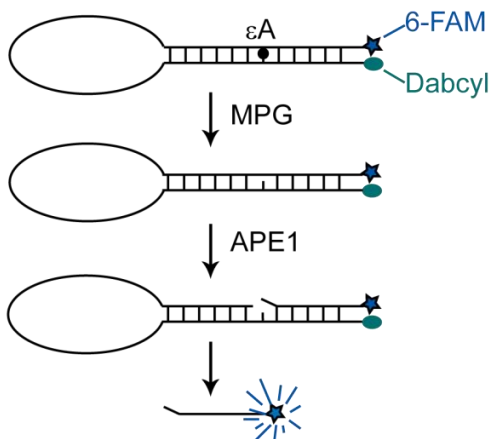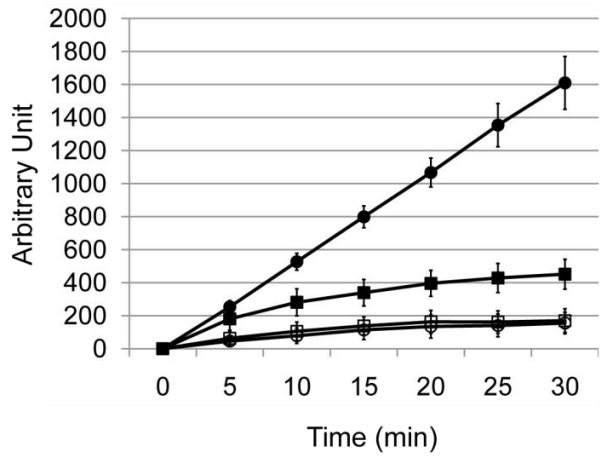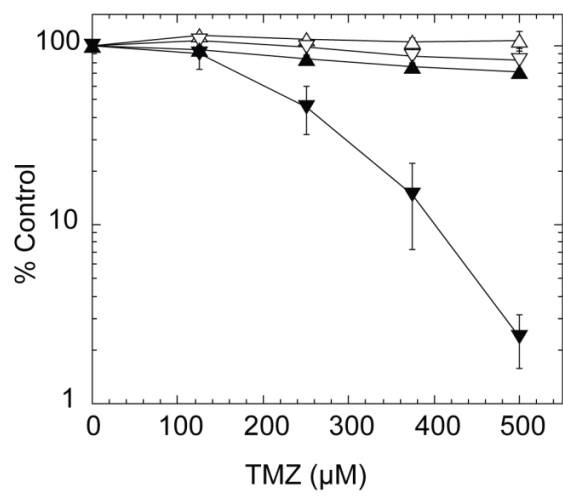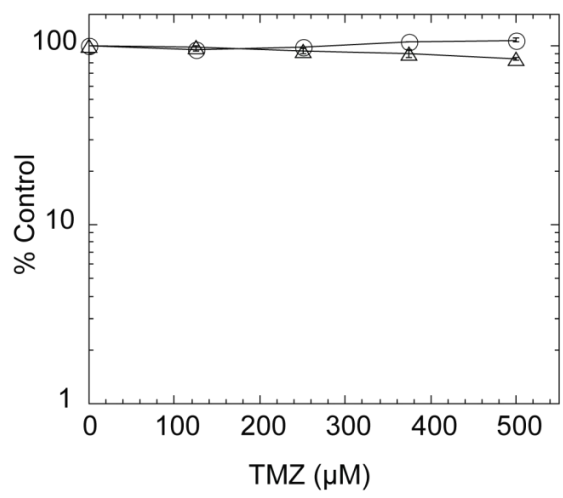**Figure 3.1 Over-expression of MPG in LN428 cells dramatically increases MX-induced potentiation of TMZ.**

(A) MPG over-expression as determined by immunoblot analysis of nuclear proteins isolated from the LN428 or LN428/MPG cells. Expression levels of the BER proteins Polß and APE1 are also shown here. PCNA expression is shown as a loading control.

(B) MPG over-expression as determined by qRT-PCR analysis of RNA isolated from LN428 and LN428/MPG cells.

(C) A schematic diagram showing the mechanism of the molecular beacon assay that is used in measuring the glycosylase activity of MPG.

(D) Increased glycosylase activity in MPG over-expressing LN428/MPG cells as determined by the molecular beacon glycosylase activity assay. Results are reported as the mean fluorescence response unit of three independent experiment ± S.E.M.

(E) MPG over-expression increases MX-induced potentiation of TMZ in LN428 cells. LN428 cells (white triangle) or LN428/MPG cells (inverted white triangle) were cultured in 96-well plates for 24 hours prior to exposure to MX (filled symbols). Following exposure to MX (60 mM) for 30 minutes, cells were treated with TMZ together with MX (30 mM) for 48 hours. Viable cells were determined using a modified MTT assay. Plots show the % viable cells as compared to untreated (control) cells. Means are calculated from quadruplicate values in each experiment. Results indicate the mean ± S.E.M. of three independent experiments.

(F) Over-expression of the glycosylase inactive MPG mutant (N169D) in LN428 cells does not increase MX-induced potentiation of TMZ. 24 hours after seeding into 96-well plates, LN428 cells over-expressing mutant MPG (N169D) were treated with (triangle) or without (open circle) MX (60 mM) for 30 minutes. Following MX pre-treatment, cells were exposed to TMZ in the presence (triangle) or absence (open circle) of MX (30 mM) for an additional 48 hours. Viable cells were counted and results were reported as in Figure 3.1E.

sensitivity to TMZ (IC_{50}, TMZ treatment: 1.5 mM; TMZ + MX treatment: 1.0 mM). However, the potentiation of TMZ induced by MX was 2 times higher in the LN428/MPG cells than in the LN428 cells as the IC_{50} was 0.8 mM and 0.25 mM for TMZ treatment or TMZ + MX treatment, respectively (**Figure 3.1E & Figure 3.5**). To confirm that MPG over-expression-induced potentiation is a result of elevated glycosylase activity, I over-expressed a mutant MPG (N169D), which has been shown to have 100-fold less glycosylase activity than the WT MPG (139), in the glioma cell line LN428 (85). Over-expression of the mutant MPG did not sensitize LN428 cells to a combined treatment of MX and TMZ (**Figure 3.1F**), which supports our hypothesis that MPG over-expression-induced sensitization is due to increased glycosylase activity in the cells.

5.2.2　MX-induced potentiation of TMZ is regulated by the expression of Polß

Although MX reacts efficiently with AP sites *in vitro* (86), it is also possible that a proportion of the AP sites produced in cells following TMZ exposure will be processed by APE1 and subsequent steps of BER *in vivo*. To investigate the impact of AP site processing by BER proteins on MX-induced potentiation of TMZ, I over-expressed Polß, the rate-limiting enzyme of the BER pathway (140), and assayed MX-induced potentiation. Over-expression of WT Polß in the LN428/MPG cells (**Figure 3.2A**) completely abrogated the potentiation induced by MX (**Figure 3.2B**, compare to Figure 3.1E). In contrast, over-expression of a 5'dRP lyase null mutant (K72A) (141, 142) of Polß (**Figure 3.2B**) did not affect MX-induced potentiation of TMZ (**Figure 3.2C**). Further, to determine whether increased expression of APE1 affects MX-induced potentiation of TMZ, I over-expressed APE1 in the LN428/MPG cells (**Figure 3.2D and Figure 3.6B**). Interestingly, increased expression of APE1 did not alter the potentiation of TMZ induced by MX (**Figure 3.2E**). A possible explanation for this observation is that although over-expression of APE1 increased its mRNA level by 20-fold, its protein level has only been slightly increased, which might not be able to significantly increase the number of AP sites processed by APE1 (see **Figure 3.2D and Figure 3.6B**).

5.2.3　PARG deficiency-induced potentiation of TMZ is enhanced by over-expression of MPG in the presence of MGMT

Next, I addressed chemotherapy sensitization in an MGMT positive background. The LN428 cell line used in our study has no detectable expression of MGMT (**Figure 3.3A**) as a result of epigenetic silencing by promoter methylation (**Figure 3.6A**). To study BER inhibition-induced

Figure 3.2

A

B

C

D

E

52
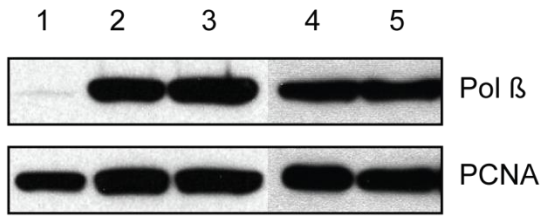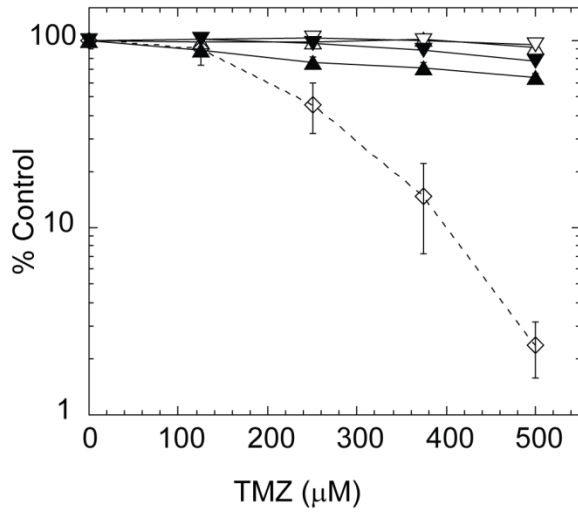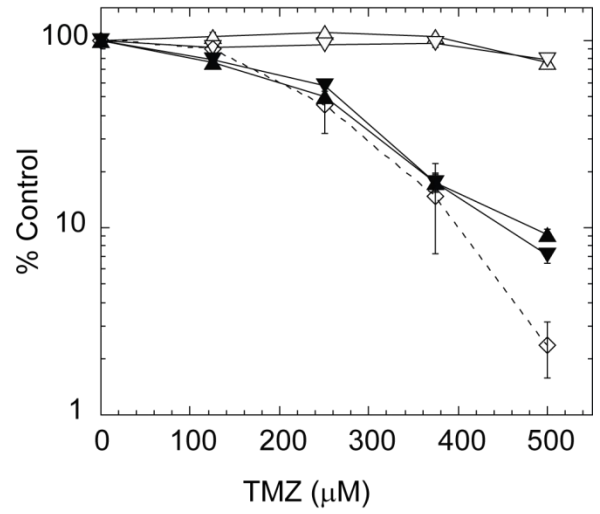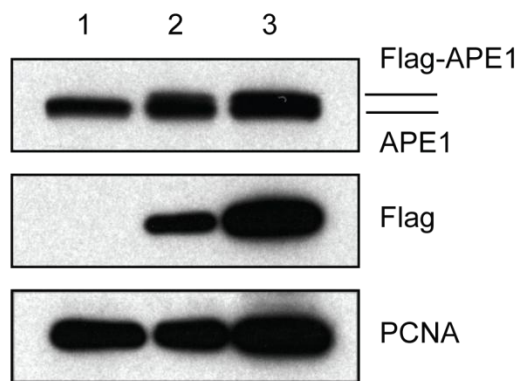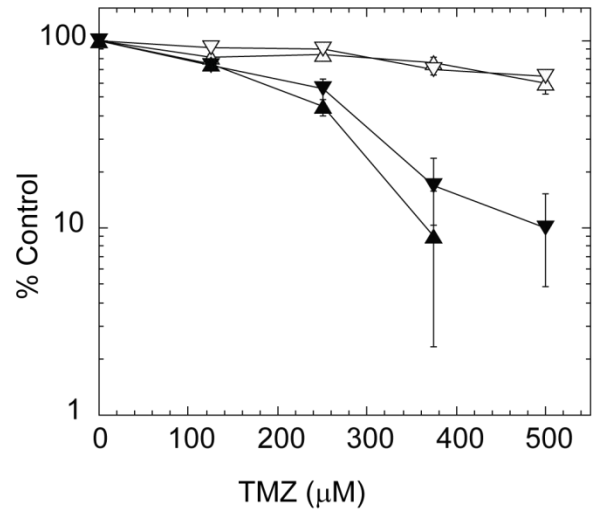
Figure 3.2 Over-expression of the BER protein Polß but not APE1 reverses MX-induced potentiation of TMZ in LN428/MPG cells.
(A) Over-expression of WT Polß or the lyase activity null mutant (K72A) of Polß in LN428/MPG cells as determined by immunoblot analysis of nuclear protein extracted from LN428/MPG/VC (vector control, lane 1), LN428/MPG/Flag-Polß-WT (clone 1 and 6 expressing Flag-tagged WT Polß, lane 4 &5), and LN428/MPG/Flag-Polß-K72A (clone 5 and 16 expressing Flag-tagged mutant Polß, lane 2 &3) cells. PCNA is shown as a loading control.
(B) Over-expression of Polß reverses MX-induced potentiation of TMZ in LN428/MPG cells. Cell viability assays were performed and results were reported as in Figure 3.1E. LN428/MPG/Flag-Polß-WT clone 1 (triangle), LN428/MPG/Flag-Polß-WT clone 6 (inverted triangle), cells treated with TMZ only (open symbols), cells treated with TMZ and MX (filled symbols). Dotted line with diamond symbols shows LN428/MPG cells treated with MX and TMZ as shown in Figure 3.1E.
**(C)** Over-expression of mutant Polß (K72A) does not reverse MX-induced potentiation of TMZ in LN428/MPG cells. Cell viability assays were performed and results were reported as in Figure 3.1E. LN428/MPG/Flag-Polß-K72A C5 (triangle), LN428/MPG/Flag-Polß-K72A C16 (inverted triangle), cells treated with TMZ only (open symbols), cells treated with TMZ and MX (filled symbols). Dotted line with diamond symbols shows LN428/MPG cells treated with MX and TMZ as shown in Figure 3.1E.
(D) Immunoblot shows over-expression of Flag tagged APE1 in the LN428/MPG cells. Lane 1: LN428/MPG/vector control; lane 2: LN428/MPG/Flag-APE1 clone 4; lane 3: LN428/MPG/Flag-APE1 clone 8. PCNA was used as a loading control.
(E) Over-expression of APE1 does not reverse MX-induced potentiation of TMZ in LN428/MPG cells. Cell viability assays were performed and results were reported as in Figure 3.1E. LN428/MPG/Flag-APE1 C4 (triangle), LN428/MPG/Flag-APE1 C8 (inverted triangle), cells treated with TMZ only (open symbols), cells treated with TMZ and MX (filled symbols).

chemotherapy potentiation in the presence of MGMT expression, the LN428 and LN428/MPG

cells were transfected with a mammalian expression plasmid (pIRES.Puro.hMGMT) and cell

clones stably expressing MGMT were selected for further analysis (**Figure 3.3B**). Over-

expression of MGMT yielded LN428 cells resistance to TMZ in a long-term cell survival assay

(**Figure 3.3C**).

Although poly(ADP-ribosyl)ation of PARP1 and other BER proteins facilitates the repair

of base lesions, the dynamics between PAR synthesis and degradation is also important for the

effectiveness of the repair process (82). Previously, it has been reported that a deficiency in the

degradation of PAR negatively affects the repair of base lesions and sensitized cells to base

Figure 3.3
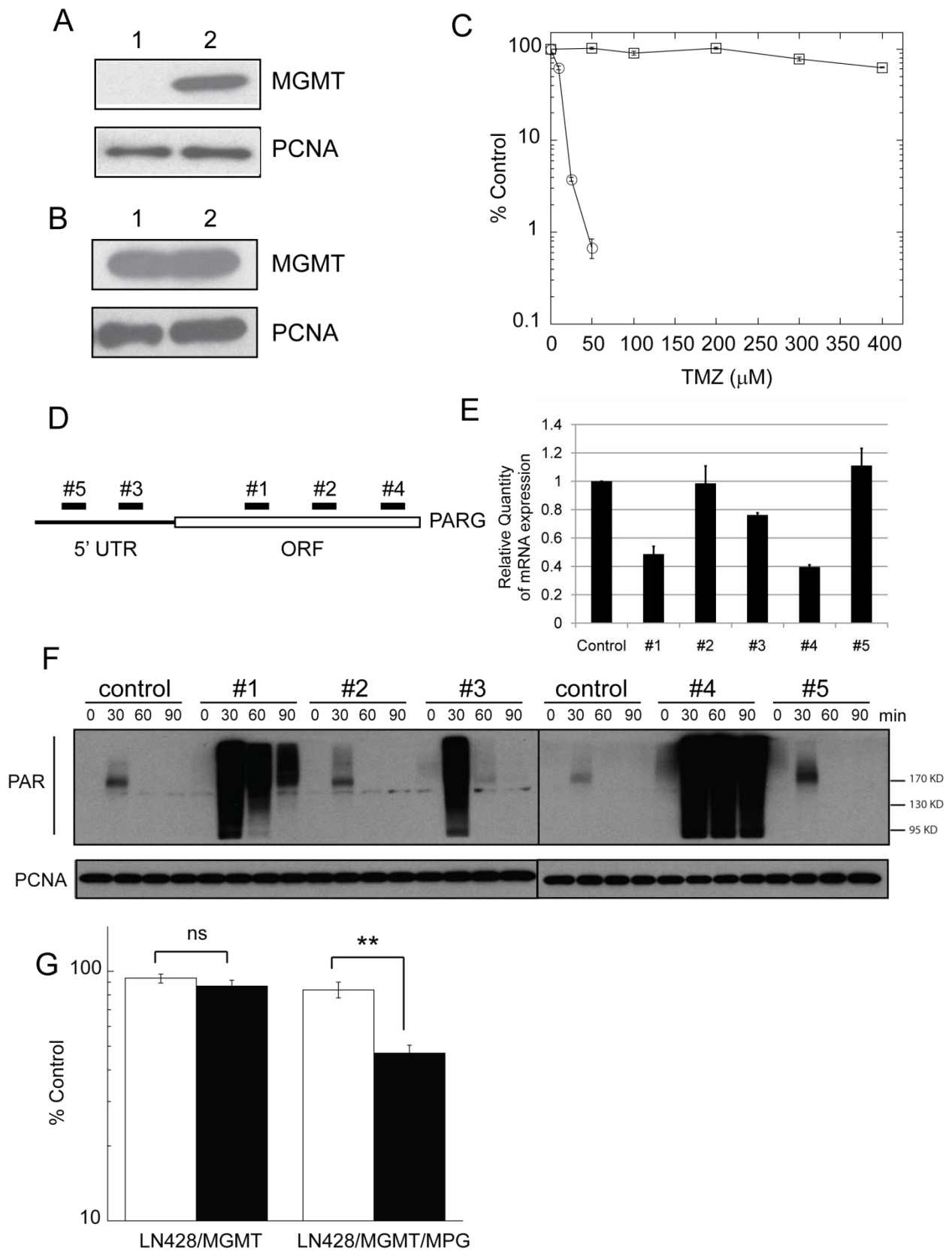
Figure 3.3 Over-expression of MPG increases PARG-KD-induced potentiation of TMZ in LN428/MGMT cells.
(A) MGMT expression as determined by immunoblot analysis of nuclear protein isolated from LN428 cells (lane 1) and T98G cells (lane 2; used as a positive control). PCNA expression is shown as a loading control. (Thanks to Dr. Ram Trivedi for performing the immunoblot analysis.)
(B) MGMT over-expression as determined by immunoblot analysis of nuclear proteins isolated from LN428 cells over-expressing MGMT (lane 1) and T98G cells (lane 2; used as a positive control). PCNA expression is shown as a loading control. (Thanks to Dr. Ram Trivedi for making the MGMT over-expression LN428 cell lines and performing the immunoblot analysis.)
(C) Over-expression of MGMT provided the sensitive LN428 cells resistance to TMZ. Cell viability assays were performed and results were reported as in Figure 3.1E. LN428, empty circle; LN428/MGMT, empty rectangle.
(D) A schematic diagram shows the five PARG shRNA constructs targeting PARG mRNA.
(E) Decreased PARG mRNA expression levels induced by the five shRNA constructs targeting PARG. Results are reported as the mean ± SE of three independent qRT-PCR experiments.
(F) PARG-KD induces delayed degradation of PAR in LN428/MPG cells following exposure to 1.5 mM TMZ as demonstrated by immunoblot analysis.
(G) PARG-KD (PARG-KD, black columns; control, white columns) significantly reduced cell survival following exposure to 300 μM TMZ in cells over expressing MPG (LN428/MGMT/MPG) as determined by long-term cell survival assay and sensitization was not statistically significant (ns) in LN428/MGMT cells with a low level of MPG expression.

damage (88). Since PARG is the primary enzyme responsible for degrading PAR *in vivo*, in this study, I investigated whether depletion of PARG-induced potentiation of TMZ can be enhanced by over-expression of MPG. I first screened five different shRNA constructs targeting PARG (**Figure 3.3D and APPENDIX B**) using a HIV-lentiviral system (104, 105) in the LN428/MPG cells for effective depletion of the enzyme. Using RNA prepared from LN428/MPG cells expressing each of the five PARG-specific shRNAs, qRT-PCR results showed that the cells expressing shRNA#1 and shRNA#4 have the lowest levels of PARG mRNA (**Figure 3.3E**). To assay the impact of PARG shRNA expression on the ability of cells to degrade DNA damage-induced PAR formation, control cells and cells treated with 1.5 mM TMZ were lysed at different time points and the lysates were probed for PAR in immunoblot analyses. Consistent with the qRT-PCR results, expression of PARG shRNA #1 and #4 greatly decreased the degradation of

Figure 3.4

A

B

C

D
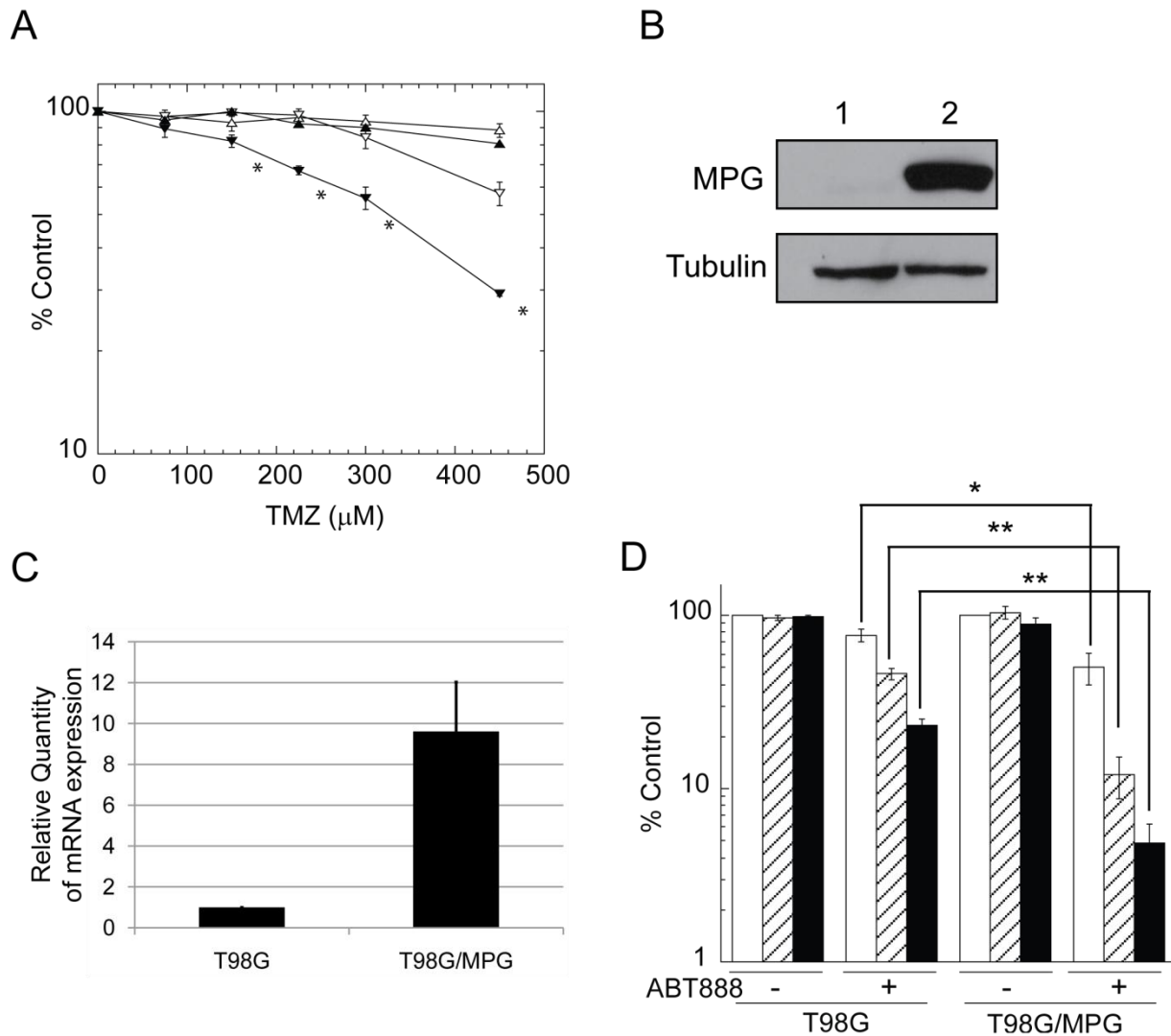
Figure 3.4 Over-expression of MPG increases PAPR inhibitor-induced potentiation of TMZ in glioma cells expressing MGMT.
(A) PJ34 significantly sensitized the MPG over-expression cells (LN428/MGMT/MPG), but not the LN428/MGMT cells to TMZ as measured by long-term cell survival assays. Triangle, LN428/MGMT cells; reversed triangle, LN428/MGMT/MPG cells; empty symbols, TMZ treatment only; filled symbols, PJ34 and TMZ treatment. Results were calculated as percentage survival relative to non-TMZ treated control cells (% Control) and reported as the mean ± S.E.M. of three independent experiments (*, p < 0.01, student t test).
(B) Over-expression of MPG in T98G cells as shown by Immunoblot. T98G, lane 1; T98G/MPG, lane 2. Tubulin was used as a loading control.
(C) Over-expression of MPG mRNA in T98G cells as shown by qRT-PCR.
(D) Over-expression of MPG in T98G cells significantly increased ABT-888-induced potentiation of TMZ as measured by long-term cell survival assays. White bars, no TMZ

treatment controls; lined bars, 50 μM TMZ treatment; black bars, 100 μM TMZ treatment. Results were calculated and reported as in Figure 3.4A. Statistics, student-t test, *: p < 0.05; **: p < 0.01.

Figure 3.5

Figure 3.5 MPG over-expression increases MX-induced potentiation of TMZ.

LN428 cells (white triangle) or LN428/MPG cells (inverted white triangle) were cultured in 96-well plates for 24 hours prior to exposure to MX (filled symbols). Following exposure to MX (60 mM) for 30 minutes, cells were treated with TMZ together with MX (30 mM) for 48 hours. Viable cells were determined using a modified MTT assay. Plots show the % viable cells as compared to untreated (control) cells. Means are calculated from quadruplicate values in each experiment. Results indicate the mean ± S.E.M. of three independent experiments.

PAR following exposure to TMZ (**Figure 3.3F**). Based on these results, I decided to use shRNA #4 for effective PARG KD in the following experiments. Further, to target tumor cells that express MGMT, I assayed PARG KD-induced potentiation of TMZ in the LN428 cell lines with over-expressed MGMT. First, I generated stable PARG KD in the MGMT expressing LN428 and LN428/MPG cell lines as determined by qRT-PCR using the PARG shRNA #4 lentivirus (**Figure 3.6C, D**). Next, using long-term cell survival assays, I probed PARG KD-induced potentiation of TMZ in these cell lines. The results demonstrated that a deficiency in degrading PAR as a result of PARG KD significantly ($p < 0.005$) sensitized cells to TMZ (300 μM) in the MPG over-expressing cells (LN428/MGMT/MPG) by decreasing % cell viability from 87% to 47% (**Figure 3.3G**), while sensitization by PARG KD was not statistically significant ($p > 0.1$) in the parental cells that exhibit a low (almost undetectable) level of MPG expression (LN428/MGMT) (**Figure 3.3G**).

5.2.4 PARP inhibitor-induced potentiation of TMZ is enhanced by over-expression of MPG in the presence of MGMT

Using a long-term cell survival assay, I next assessed if PARP inhibitor-induced potentiation of TMZ is affected by over-expression of MPG. I have previously shown that the PARP inhibitor PJ34 (2 μM) significantly reduced the level of PARP activation following exposure to TMZ (85). Here I show that pre- (4 μM) and co-treatment with PJ34 (2 μM) significantly sensitized cells to TMZ, with $p < 0.01$ for TMZ doses higher than 150 μM, and sensitization by PJ34 was not observed in the parental cells with a low level of MPG expression (LN428/MGMT) (**Figure 3.4A**). To further confirm that over-expression of MPG increases PARP inhibition-induced potentiation of TMZ in glioma cells, I used a second glioma cell line T98G (143), which has
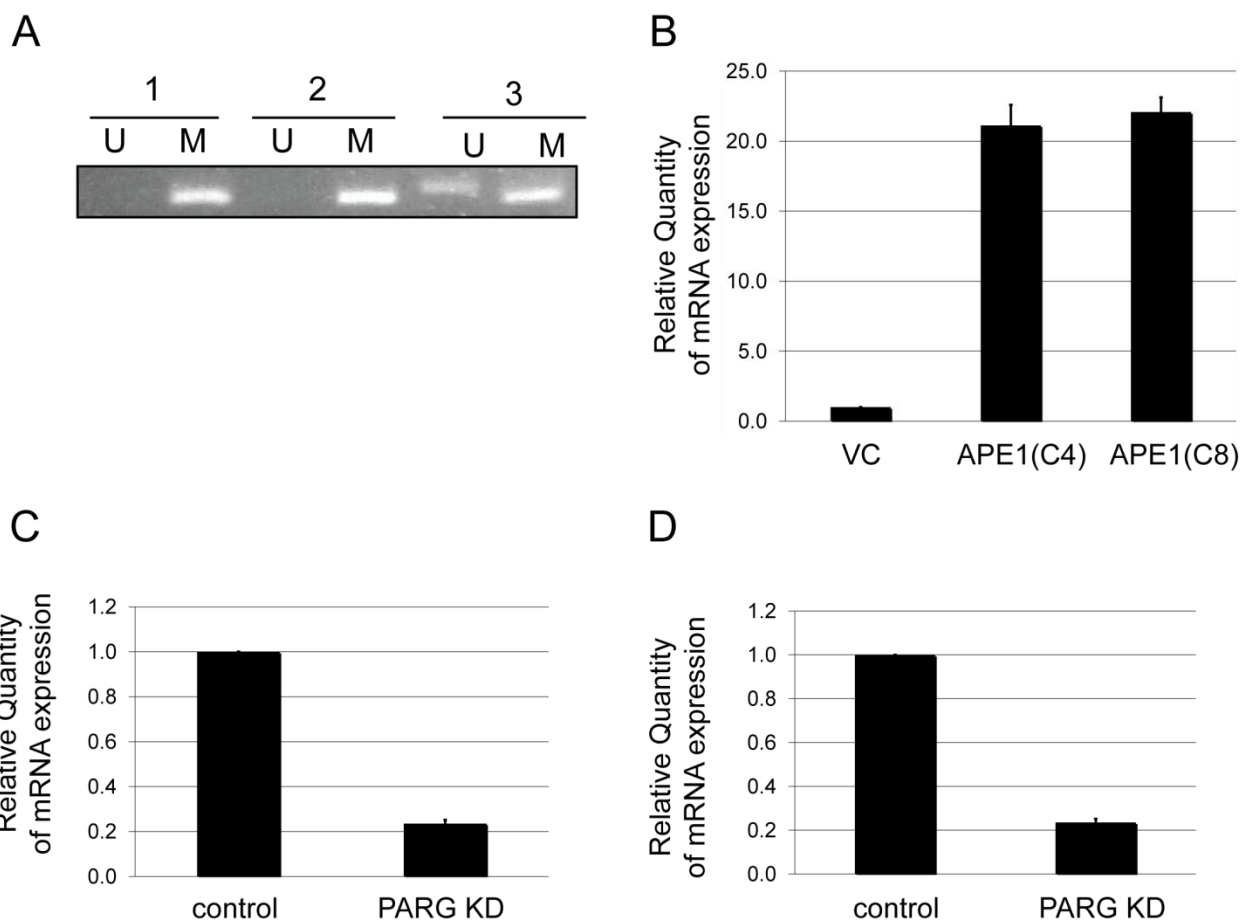
Figure 3.6 Cell line characterization
(A) MGMT promoter methylation analysis of Bisulfite-treated DNA used for PCR in the DNA extracted from LN428 cells (Group 2, U: unmethylated and M: methylated), T98G cells (Group 3, U: unmethylated and M: methylated), Universal unmethylated DNA as a negative control DNA (Group 1, U: unmethylated) and Universal methylated DNA as a positive control (Group 1, M: methylated). (The assay was performed by Xiao-hong Wang, Dr. Robert Sobol's laboratory.)
(B) Over-expression of APE1 in LN428/MPG cells as shown by qRT-PCR. Two clones were shown here, C4 and C8.
(C & D) qRT-PCR results showing PARG KD in MGMT over expressing LN428/MGMT (C) and LN428/MPG/MGMT (D) cells. Results are reported as the mean ± SE of three independent experiments.

endogenously elevated expression of MGMT (**Figure 3.3A, B**). I inhibited BER using the

clinically utilized PARP inhibitor ABT-888 in similar experiments as those conducted in the

LN428 cell lines. I first over-expressed MPG in the T98G cells using a mammalian expression

plasmid (pRS1422). Over-expression of MPG in the T98G cells increased its mRNA level (10-fold) and protein level as determined by immunoblot and qRT-PCR analysis (**Figure 3.4B, C**). Consistent with previous reports that demonstrate ABT-888 potentiates TMZ in diverse tumor models (98, 144), treatment with ABT-888 sensitized T98G cells to TMZ (**Figure 3.4D**). More importantly, over-expression of MPG significantly increased the potentiation induced by ABT-888 (**Figure 3.4D**, $p < 0.05$ and $p < 0.01$). These results demonstrate that increased base repair initiation enhances PARP inhibitor-induced potentiation of TMZ, suggesting that combining an increase in repair initiation and BER inhibition is an effective way to improve chemotherapeutic efficacy and the expression level of MPG in tumors might be used as a biomarker to predict effectiveness of alkylator chemotherapy potentiation.

6.0   DISCUSSION

6.1   PARP ACTIVATION DEPENDENT CELL DEATH IN RESPONSE TO DNA

BASE DAMAGE

The requirement for BER in general and Polß more specifically in the repair of genomic DNA base damage, particularly DNA damage induced by alkylating agents such as the chemotherapeutic TMZ and the SN1 & SN2 alkylating agents MNNG and MMS, respectively (51, 57), elevates the significance of characterizing the mechanism responsible for Polß deficiency-induced cell death [e.g., a failure to complete repair of the BER intermediate 5'dRP in the absence of Polß]. As evidenced recently by the development of clinically significant PARP inhibitors, identifying BER proteins critical for response to DNA damaging agents (e.g., chemotherapy) can have broad human health implications. Equally important is a clear understanding of the mechanism(s) that contribute to the enhanced cell death observed upon DNA repair inhibition. For example, PARP inhibition triggers apoptosis via the accumulation of DSBs (59, 60) and a requirement for HR proteins such as BRCA1 and BRCA2 (45). To this end, I have developed a unique series of genetically modified human tumor cell lines as models of Polß deficiency that accumulate the cytotoxic BER intermediate 5'dRP following exposure to alkylating agents (TMZ, MMS and MNNG). By directly comparing the cellular, biochemical and signaling responses to DNA base damage in BER defective (Polß deficient) and BER competent

isogenic human cell lines, these responses can be defined as either global (non-specific) or BER (Polß) specific effects, the latter resulting from a cellular response to the inability to complete BER, referred to herein as "**BER Failure**". I have then utilized this system to define the mechanism of cell death resulting from Polß loss/inhibition or BER failure and propose and test paradigms to enhance the cell death response.

From these studies, I find that the un-repaired BER intermediates that accumulate upon DNA damaging agent exposure when Polß is deficient will activate PARP1, leading to a rapid onset of PARP1-dependent, caspase-independent cell death with little or no role for a caspase-dependent or autophagy-dependent process in the response. It remains to be determined if the BER failure-induced cell death observed herein is dependent on ERK1/2–mediated PARP1 phosphorylation (145), SIRT1-regulated deacetylation of PARP1 (146) or if the observed PARP1-induced cell death requires BAX, Calpain and JNK activation (147). Coincident with damage-induced necrosis in Polß deficient cells is PARP1-dependent HMGB1 secretion (119), a hallmark of caspase-independent cell death and inflammation signaling. HMGB1 functions in the extra-cellular space as a robust RAGE ligand and inflammatory cytokine or damage-associated molecular pattern molecule (118), suggesting that BER failure and the resulting PARP1 activation may trigger an inflammatory response in tissues with a BER imbalance such as ulcerative colitis (148).

There are multiple PARP1-activation induced cell death mechanisms, as outlined in the diagram shown in **Figure 2.5A**. In one, it is suggested that PAR, the product of PARP1 activation, is a cell death molecule. In this process, PAR initiates the translocation of AIF from the mitochondria to the nucleus by a RIP1-dependent mechanism (35, 64, 65, 121) (**Figure 2.5A**). Uniquely, PAR generated due to BER failure does not appear to trigger cell death via

RIP1 activation nor does PAR function as a signal to initiate AIF translocation. PARP1 is involved in many DNA repair processes including homologous recombination (HR) and non-homologous end joining (NHEJ) in response to DSBs and has a role in telomere maintenance (32, 33). The question remains if PAR generated via BER failure is of a unique chemical make-up as compared to PAR generated from DSB-induced PARP1 activation. One possible explanation for the absence of a role for AIF in this study is the concentration of DNA damaging agents used. In this report, we have used TMZ or MMS at a maximum concentration of 1.5 mM or MNNG at a concentration of 5 μM, resulting in 90-95% cell death in the BER deficient cells with little or no cell death in the control cells (**Figure 2.8A**). Many reports of PAR-induced AIF translocation include MNNG concentrations of 100 and 500 μM (147, 149, 150). Such high concentrations of DNA damaging gents (e.g., MNNG at 20X and 100X that used herein) have the potential to directly induce DNA DSBs, create overwhelming levels of both nuclear and mitochondrial genome damage (151) as well as the possibility of direct protein alkylation. Regardless, it is clear that the cell death initiated by BER failure is independent of RIP1 activation and AIF translocation, thus ruling out PAR as the cell death signal that is initiated upon BER failure.

One explanation for the absence of PAR-mediated cell death is the rapid catabolism of PAR by PARG (127). In this study, I find that PAR synthesized due to PARP activation is degraded within 90 minutes (**Figure 2.2**). As summarized in **Figure 2.5A**, the breakdown products of PAR (PAR catabolites) are also likely mediators of cell death, including ADP-ribose (activator of the Ca^{2+} channel TRPM2) and AMP (inhibitor of ATP transport) (66-68). However, PARG knockdown did not reverse the DNA damage-sensitive phenotype of Polß deficient cells (**Figure 2.6C**), suggesting that damage-dependent cell death in Polß deficient cells is not

initiated by PAR catabolites. Conversely, the PAR catabolite AMP may provide a protective phenotype by activation of AMPK, induction of autophagy and enhanced ATP synthesis, as recently reported following ROS-induced DNA damage and PARP1 activation (152). Although loss of AMPK activation and induction of autophagy upon PARG-KD could explain, in part, the enhanced cell death observed in the PARG-KD cells (**Figure 2.6C**), we suggest this is unlikely, since in this study, autophagy is not involved (**Figure 2.4B**) and the activation of AMPK, if any, does not appear to overcome the damage-induced cell death phenotype resulting from BER failure in the PARG proficient cells. Regardless, it is interesting to speculate that PARG may regulate AMPK activation in response to ROS-induced PARP1 activation (152). In all, these studies imply that the alkylation-sensitive phenotype of Polß deficient cells is un-related to the accumulation of PAR catabolites such as ADP-ribose or AMP and is likely wholly dependent on the metabolite bioavailability or bioenergetic capacity of the cell.

The over-riding response to the loss of Polß and an inability to complete BER (BER failure) is energy failure or depletion of bioenergetic metabolites with no evidence for cell death triggered by PAR or the PAR catabolites ADP-ribose or AMP. The energy collapse or depletion of NAD^+ and ATP due to BER failure is offset by elevated levels of NMN (136) and is negatively affected by NAD^+ biosynthesis inhibition (FK-866), suggesting that *(i)* FK-866 (APO866) and related clinically useful NAD^+ biosynthesis inhibitors might be combined with TMZ and BER inhibitors to improve TMZ response and *(ii)* any stress on or defects in the NAD^+ biosynthesis pathway such as over-activation of SIRT1 (153) or attenuating defects in NAMPT, NMNAT1 or related NAD biosynthetic enzymes (154) may have significant effects on cell survival following BER failure.

Similar phenotypes (stress-induced PARP1 activation and cell survival dependent on NAD^+ metabolites) have been observed in diverse human cell types and mammalian organ systems, stressing the significance of these findings. PARP1 activation and the resulting "NAD^+ depletion"-mediated or ATP-depletion mediated cell death plays a critical role in tissue injury from cerebral and myocardial ischemia (114, 115, 155, 156). Analogous to the studies described herein, cellular protection from cerebral ischemia is provided by NAD^+ metabolite supplementation (157, 158). Similarly, streptozotocin-induced diabetes results from PARP1 activation, energy imbalance and cell death dependent on the BER enzyme MPG (159-162). Most importantly, cellular NAD^+ metabolism plays an essential role in pancreatic ß-cell viability and insulin secretion (163). With the observation that BER failure triggers NAD^+ depletion, it is interesting to speculate if overall BER capacity controls susceptibility to ischemia or streptozotocin-induced and age-related diabetes onset via neuronal or ß-cell death from loss of bioenergetic metabolites subsequent to BER failure. The onset of these physiologically significant outcomes (stroke, neurodegeneration, ischemia, diabetes) involves PARP1 activation, NAD^+ depletion and cell death, similar to that reported here. Although a portion of the environmental and endogenous stressors that induce these phenotypes via PARP1 activation will directly induce DNA single-strand breaks, it is reasonable to presume that a significant proportion of cell death related to stroke, retinal degeneration, ischemia and diabetes may initiate from genomic DNA base damage, requiring repair by the BER machinery. As such, the failure to repair the DNA damage and the resulting accumulation of DNA repair intermediates (BER failure) may be the trigger of PARP1 activation and cell death.

In summary, these studies suggest that PARP1 functions as a BER molecular sensor protein to induce caspase-independent cell death following BER failure and provides mechanistic insight into why Polß deficiency leads to cell death. Further, these studies demonstrate that the observed DNA damage dependent cell death in Polß deficient cells is unrelated to the accumulation of PAR catabolites such as ADP-ribose or AMP yet is dependent on NAD^+ metabolite bioavailability or bioenergetic capacity of the cell, suggesting a linkage between DNA repair capacity, cell survival and cellular bioenergetic metabolites. Finally, these studies have potentially important implications for therapeutic development as it relates to a chemotherapy-induced synthetic lethality approach to cancer therapy involving the combination of a chemotherapeutic DNA damaging agent, a DNA repair inhibitor and a regulator or inhibitor of NAD^+ biosynthesis.

6.2   EXPRESSION OF MPG DRIVES BER INHIBITION-INDUCED CHEMOTHERAPY SENSITIZATION

As the first enzyme in the BER pathway for the repair of alkylated bases, glycosylase activity of MPG is required for the initiation of BER to repair a spectrum of lesions, including 3MeA and 7MeG (76). It has been demonstrated that MPG expression levels vary considerably in human breast cancer (164), astrocytic tumors (165) and glioblastoma. In addition, MPG possesses multiple post translational modifications and interacts with many DNA repair proteins, including XRCC1 and hR23A, suggesting that the glycosylase activity of MPG may be under tight cellular regulation (53). Here, I demonstrate that BER inhibition-mediated sensitization of glioma cells to the chemotherapeutic agent TMZ is further increased by enhancing BER repair initiation via

over-expression of MPG. Glioma cells with elevated-expression of MPG exhibited dramatically increased potentiation of TMZ via BER inhibition by MX, the PARP inhibitors PJ34 and ABT-888 or by PARG depletion (PARG-KD). The enhanced potentiation of TMZ in the MPG over-expressing glioma cell lines observed in these studies is in-line with a previous report showing that MX-induced sensitization is increased by MPG over-expression in ovarian cancer cells (49). However, the expression level of MPG is not the only factor that controls MX-induced potentiation of TMZ, as it is also related to the efficiency and balance of the BER pathway proteins that process AP sites and downstream repair intermediates. From these experiments (**Figure 3.2B & C**), it is demonstrated that over-expression of the wild type BER rate-limiting enzyme Polß but not the 5'dRP lyase activity null mutant of Polß (K72A), in the MPG over-expressing cells, abrogates the MPG dependent potentiation of TMZ. Therefore, it is the collective expression status of both MPG and Polß that defines the sensitization induced by MX. APE1 is the main enzyme that directly competes with MX for the processing of AP sites in cells, yet over-expression of the enzyme did not alter MX-induced potentiation of TMZ (**Figure 3.2E**). A possible explanation might be that although APE1 mRNA level was increased by more than 20X (**Figure 3.6B**) the protein level of APE1 was only slightly increased (**Figure 3.2D**). Since APE1 is an abundant enzyme in cells, a slight increase of the protein level of APE1 may not change the rate of AP sites processed by APE1 or MX.

According to our previous study, the dynamics between PAR synthesis and degradation are not only involved in facilitating repair of base lesions, but also acts as a mediator of cell death via hyperactivation of PARP and subsequent cellular energy depletion in response to accumulation of un-repaired BER intermediates (85). Thus, although inhibition of PARP hyperactivation and PAR synthesis provides short-term cell survival advantage, it is very likely

that damage-induced DNA lesions persist in cells due to inhibition of PARP. Cells harboring the un-repaired DNA lesions will eventually die due to accumulation of DSBs as cells go through replication. Therefore, in the context of chemotherapy sensitization involving PARP inhibition or depletion of PARG (PARG KD), the long-term assay (10 days) for cell survival, which allows for multiple rounds of DNA replication, is more suitable than the short-term (2 days) MTS assay. For the reason stated above, all the cell survival assays involving PARG or PARP inhibition were conducted using the long-term assay as described in the Materials and Methods section.

PARG is the primary enzyme for degrading PAR in human cells. It has been reported that the PARG inhibitor GPI 16552 chemosensitizes malignant melanoma to TMZ (82), which implies that not only poly(ADP-ribosyl)ation of target proteins by PARP but also the rapid clearance of PAR by PARG is important for cell survival following DNA base damage. Contradictory to the previous report demonstrating that PARG inhibition sensitizes melanoma to TMZ (82), these studies demonstrate that shRNA-mediated PARG-KD did not significantly (p > 0.1) sensitize the LN428/MGMT cells to TMZ. However, I found that the sensitization is significant (p < 0.005) in cells with over-expression of MPG (**Figure 3.3G**).

PARP has recently become the focus of investigations of chemotherapy potentiation since the publication of a sensitive phenotype induced by PARP inhibitors in breast cancer cells bearing a loss of BRCA1 or BRCA2 function (166, 167). Currently, PARP inhibitors are under phase 0 to phase 2 clinical trials in combination with the clinical alkylating agent TMZ (89). The rationale for combining a PARP inhibitor with TMZ is generally considered to be inhibition of repair of TMZ-induced DNA lesions via inhibiting PARP. However, it is not known if the status of the BER pathway inherent in cancer cells has an impact on the potentiation induced by PARP inhibitors. In this study, using the PARP inhibitors PJ34 and ABT-888, these studies demonstrate

that PARP inhibition-induced potentiation of TMZ is significantly enhanced in glioma cells with elevated expression of MPG (**Figure 3.4A, D**), suggesting that increased repair initiation of TMZ-induced base lesions can further sensitize cancer cells to PARP inhibition and that the expression level of MPG in cancer cells may predict clinical benefit of PARP inhibitors in combination with TMZ.

This study addresses the relationship between DNA glycosylase expression and chemotherapy sensitization via BER inhibition (MX, the PARP inhibitors PJ34 and ABT-888 or PARG-KD). These studies demonstrate that BER inhibition-induced potentiation of TMZ is enhanced by over-expression of the BER initiating enzyme MPG, suggesting that combining an increase in repair initiation and inhibition of repair following initiation of the BER pathway is an effective means to improved chemotherapy efficacy. Further these studies suggest that the expression level of MPG in cancer cells might be used to predict effectiveness when combining BER inhibition and alkylating agents.

APPENDIX A

CELL LINES DEVELOPED AND USED IN 5.1

Cell line name	Clone #	Cell line description	Growth media
LN428	-	Human glioma cell line	Alpha EMEM, heat-inactivated fetal bovine serum (10%), glutamine (2 mM), antibiotic & antimycotic, gentamicin (50 μg/ml).
LN428/Pol ß KD	-	LN428 cells expressing Polß shRNA and copGFP	LN428 cell growth media
LN428//MPG	7	LN428 cells modified for over-expression of human MPG	LN428 cell growth media + 600 μg/ml neomycin
LN428//MPG/ Pol ß KD	-	LN428 cells modified for over-expression of human MPG, expressing Polß shRNA and copGFP	LN428 cell growth media + 600 μg/ml neomycin
LN428/MPG/GFP	-	LN428/MPG cells expressing copGFP	LN428 cell growth media + 600 μg/ml neomycin
LN428/VC*	1	LN428 cells transfected with vector control plasmid pIRES-neo	LN428 cell growth media + 600 μg/ml neomycin
LN428/MPG/VC*	2	LN428/MPG cells transfected with vector control plasmid pIRES-puro	LN428 cell growth media + 600 μg/ml neomycin + 1.0 μg/ml puromycin
LN428/MPG/Pol ß KD/VC*	3	LN428/MPG/Polß-KD cells transfected with vector control plasmid pIRES-puro	LN428 cell growth media + 600 μg/ml neomycin + 1.0 μg/ml puromycin
LN428/MPG-N169D	11	LN428 cells modified to express glycosylase dead	LN428 cell growth media + 600 μg/ml neomycin

		mutant of MPG (N169D)	
LN428/MPG/Flag-Pol ß-WT*	1	LN428/MPG cells expressing Flag tagged WT Polß	LN428 cell growth media + 600 µg/ml neomycin + 1.0 µg/ml puromycin
	6		
LN428/MPG/Flag-Pol ß-K72A	5	LN428/MPG cells expressing Flag tagged 5'dRP lyase activity dead mutant Polß	LN428 cell growth media + 600 µg/ml neomycin + 1.0 µg/ml puromycin
	16		
LN428/MPG/Pol ß KD/Flag-Pol ß-WT*	2	LN428/MPG/Pol ß KD cells expressing Flag tagged WT Polß	LN428 cell growth media + 600 µg/ml neomycin + 1.0 µg/ml puromycin
	6		
LN428/MPG/Flag-APE1	4	LN428/MPG cells over-expressing Flag tagged APE1	LN428 cell growth media + 600 µg/ml neomycin + 1.0 µg/ml puromycin
	8		
LN428/MGMT	5	LN428 cells over-expressing human MGMT	LN428 cell growth media + 1.0 µg/ml puromycin
LN428/MPG/MGMT	8	LN428/MPG cells over-expressing human MGMT	LN428 cell growth media + 600 µg/ml neomycin + 1.0 µg/ml puromycin
LN428/MGMT/PARG KD	-	LN428/MGMT cells co-expressing PARG shRNA and TurboGFP	LN428 cell growth media + 1.0 µg/ml puromycin
LN428/MPG/MGMT/PARG KD	-	LN428/MPG/MGMT cells co-expressing PARG shRNA and TurboGFP	LN428 cell growth media + 600 µg/ml neomycin + 1.0 µg/ml puromycin
T98G	-	Human glioma cell line	EMEM, FBS (10%), sodium pyruvate, MEM non-essential amino acids, antibiotic & antimycotic, gentamycin
T98G/MPG	1	T98G cells over-expressing human MPG	T98G cell growth media + 400 µg/ml neomycin

VC*: vector control.
WT*: wild type.

APPENDIX B

MISSION™ TRC SHRNA TARGET SET FOR PARG

TRC No.		ShRNA #
TRCN0000 051303	**CCGGGCTAAGATGAAATCGGAGTATCTCGAGATACTCCGATT** **TCATCTTAGCTTTTTG** Clone ID: NM_003631.1-2105s1c1 Accession Number(s): NM_003631.2 Region: CDS	**1**
TRCN0000 051306	**CCGGCGATTGCATGTCACTTACGAACTCGAGTTCGTAAGTGA** **CATGCAATCGTTTTTG** Clone ID: NM_003631.1-2315s1c1 Accession Number(s): NM_003631.2 Region: CDS	**2**
TRCN0000 051307	**CCGGGCCTAGGAAATTCTCCTCCATCTCGAGATGGAGGAGAA** **TTTCCTAGGCTTTTTG** Clone ID: NM_003631.1-1026s1c1 Accession Number(s): NM_003631.2 Region: CDS	**3**
TRCN0000 051305	**CCGGGCTGAGCGAGATGTGGTTTATCTCGAGATAAACCACAT** **CTCGCTCAGCTTTTTG** Clone ID: NM_003631.1-2843s1c1 Accession Number(s): NM_003631.2, XM_937616.2 Region: CDS	**4**
TRCN0000 051304	**CCGGGCAGTTTAGTAATGCTAACATCTCGAGATGTTAGCATTA** **CTAAACTGCTTTTTG** Clone ID: NM_003631.1-706s1c1 Accession Number(s): NM_003631.2 Region: CDS	**5**

BIBLIOGRAPHY

1.   DeVita VT, Hellman S, Rosenberg SA. Cancer, principles & practice of oncology. 7th ed. Philadelphia, PA: Lippincott Williams & Wilkins; 2005.
2.   CBTRUS. CBTRUS Statistical Report: Primary brain and Central Nervous System Tumors Diagnosed in the United States in 2004-2005. Published by the Central Brain Tumor Registry of the United States 2009 2009.
3.   Scoles DR, Pulst SM, Michael JA, Robert BD. Brain Tumors, Genetics. Encyclopedia of the Neurological Sciences. New York: Academic Press; 2003. p. 470-2.
4.   Kleihues P, Louis DN, Scheithauer BW, et al. The WHO classification of tumors of the nervous system. J Neuropathol Exp Neurol 2002; 61:215-25; discussion 26-9.
5.   Louis DN, von Deimling A, Chung RY, et al. Comparative study of p53 gene and protein alterations in human astrocytic tumors. J Neuropathol Exp Neurol 1993; 52:31-8.
6.   von Deimling A, Eibl RH, Ohgaki H, et al. p53 mutations are associated with 17p allelic loss in grade II and grade III astrocytoma. Cancer Res 1992; 52:2987-90.
7.   Liu W, James CD, Frederick L, Alderete BE, Jenkins RB. PTEN/MMAC1 mutations and EGFR amplification in glioblastomas. Cancer Res 1997; 57:5254-7.
8.   Ekstrand AJ, James CD, Cavenee WK, Seliger B, Pettersson RF, Collins VP. Genes for epidermal growth factor receptor, transforming growth factor alpha, and epidermal growth factor and their expression in human gliomas in vivo. Cancer Res 1991; 51:2164-72.
9.   Stewart LA. Chemotherapy in adult high-grade glioma: a systematic review and meta-analysis of individual patient data from 12 randomised trials. Lancet 2002; 359:1011-8.
10.   Stupp R, Mason WP, van den Bent MJ, et al. Radiotherapy plus concomitant and adjuvant temozolomide for glioblastoma. N Engl J Med 2005; 352:987-96.
11.   Yung WK, Albright RE, Olson J, et al. A phase II study of temozolomide vs. procarbazine in patients with glioblastoma multiforme at first relapse. Br J Cancer 2000; 83:588-93.
12.   Sobol RW. Temozolomide. In: Schwab M, editor. Encyclopedia of Cancer. 2nd ed. Berlin, Heidelberg, New York: Springer; 2008. p. In Press.
13.   Rinne ML, He Y, Pachkowski BF, Nakamura J, Kelley MR. N-methylpurine DNA glycosylase overexpression increases alkylation sensitivity by rapidly removing non-toxic 7-methylguanine adducts. Nucleic Acids Res 2005; 33:2859-67.
14.   Trivedi RN, Wang XH, Jelezcova E, Goellner EM, Tang J, Sobol RW. Human methyl purine DNA glycosylase and DNA polymerase {beta} expression collectively predict sensitivity to temozolomide. Mol Pharmacol 2008.
15.   Shrivastav N, Li D, Essigmann JM. Chemical biology of mutagenesis and DNA repair: cellular responses to DNA alkylation. Carcinogenesis 2010; 31:59-70.

16.   Fronza G, Gold B. The biological effects of N3-methyladenine. J Cell Biochem 2004; 91:250-7.

17.   Lindahl T, Sedgwick B, Sekiguchi M, Nakabeppu Y. Regulation and expression of the adaptive response to alkylating agents. Annu Rev Biochem 1988; 57:133-57.

18.   Kaina B, Christmann M, Naumann S, Roos WP. MGMT: key node in the battle against genotoxicity, carcinogenicity and apoptosis induced by alkylating agents. DNA Repair (Amst) 2007; 6:1079-99.

19.   Yoshioka K, Yoshioka Y, Hsieh P. ATR kinase activation mediated by MutSalpha and MutLalpha in response to cytotoxic O6-methylguanine adducts. Mol Cell 2006; 22:501-10.

20.   York SJ, Modrich P. Mismatch repair-dependent iterative excision at irreparable O6-methylguanine lesions in human nuclear extracts. J Biol Chem 2006; 281:22674-83.

21.   Sarkaria JN, Kitange GJ, James CD, et al. Mechanisms of chemoresistance to alkylating agents in malignant glioma. Clin Cancer Res 2008; 14:2900-8.

22.   Stegh AH, Chin L, Louis DN, DePinho RA. What drives intense apoptosis resistance and propensity for necrosis in glioblastoma? A role for Bcl2L12 as a multifunctional cell death regulator. Cell Cycle 2008; 7:2833-9.

23.   Stegh AH, Kesari S, Mahoney JE, et al. Bcl2L12-mediated inhibition of effector caspase-3 and caspase-7 via distinct mechanisms in glioblastoma. Proc Natl Acad Sci U S A 2008; 105:10703-8.

24.   Horton JK, Wilson SH. Hypersensitivity phenotypes associated with genetic and synthetic inhibitor-induced base excision repair deficiency. DNA Repair (Amst) 2007; 6:530-43.

25.   Gerson SL. MGMT: its role in cancer aetiology and cancer therapeutics. Nat Rev Cancer 2004; 4:296-307.

26.   Hegi ME, Diserens AC, Gorlia T, et al. MGMT gene silencing and benefit from temozolomide in glioblastoma. N Engl J Med 2005; 352:997-1003.

27.   Lindahl T. Instability and decay of the primary structure of DNA. Nature 1993; 362:709-15.

28.   Lindahl T, Wood RD. Quality control by DNA repair. Science 1999; 286:1897-905.

29.   Nakamura J, Walker VE, Upton PB, Chiang SY, Kow YW, Swenberg JA. Highly sensitive apurinic/apyrimidinic site assay can detect spontaneous and chemically induced depurination under physiological conditions. Cancer Res 1998; 58:222-5.

30.   Hou EW, Prasad R, Asagoshi K, Masaoka A, Wilson SH. Comparative assessment of plasmid and oligonucleotide DNA substrates in measurement of in vitro base excision repair activity. Nucleic Acids Res 2007; 35:e112.

31.   Almeida KH, Sobol RW. A unified view of base excision repair: lesion-dependent protein complexes regulated by post-translational modification. DNA Repair (Amst) 2007; 6:695-711.

32.   Hassa PO, Haenni SS, Elser M, Hottiger MO. Nuclear ADP-ribosylation reactions in mammalian cells: where are we today and where are we going? Microbiol Mol Biol Rev 2006; 70:789-829.

33.   Schreiber V, Dantzer F, Ame JC, de Murcia G. Poly(ADP-ribose): novel functions for an old molecule. Nat Rev Mol Cell Biol 2006; 7:517-28.

34.   Kurosaki T, Ushiro H, Mitsuuchi Y, et al. Primary structure of human poly(ADP-ribose) synthetase as deduced from cDNA sequence. J Biol Chem 1987; 262:15990-7.

35.   Yu SW, Wang H, Poitras MF, et al. Mediation of poly(ADP-ribose) polymerase-1-dependent cell death by apoptosis-inducing factor. Science 2002; 297:259-63.

36.   Koh DW, Dawson TM, Dawson VL. Mediation of cell death by poly(ADP-ribose) polymerase-1. Pharmacol Res 2005; 52:5-14.

37.   Virag L, Szabo C. The therapeutic potential of poly(ADP-ribose) polymerase inhibitors. Pharmacol Rev 2002; 54:375-429.

38.   Satoh MS, Lindahl T. Role of poly(ADP-ribose) formation in DNA repair. Nature 1992; 356:356-8.

39.   Dantzer F, de La Rubia G, Menissier-De Murcia J, Hostomsky Z, de Murcia G, Schreiber V. Base excision repair is impaired in mammalian cells lacking Poly(ADP-ribose) polymerase-1. Biochemistry 2000; 39:7559-69.

40.   Shall S, de Murcia G. Poly(ADP-ribose) polymerase-1: what have we learned from the deficient mouse model? Mutat Res 2000; 460:1-15.

41.   Masson M, Niedergang C, Schreiber V, Muller S, Menissier-de Murcia J, de Murcia G. XRCC1 is specifically associated with poly(ADP-ribose) polymerase and negatively regulates its activity following DNA damage. Mol Cell Biol 1998; 18:3563-71.

42.   Prasad R, Lavrik OI, Kim SJ, et al. DNA polymerase beta -mediated long patch base excision repair. Poly(ADP-ribose)polymerase-1 stimulates strand displacement DNA synthesis. J Biol Chem 2001; 276:32411-4.

43.   Leppard JB, Dong Z, Mackey ZB, Tomkinson AE. Physical and functional interaction between DNA ligase IIIalpha and poly(ADP-Ribose) polymerase 1 in DNA single-strand break repair. Mol Cell Biol 2003; 23:5919-27.

44.   El-Khamisy SF, Masutani M, Suzuki H, Caldecott KW. A requirement for PARP-1 for the assembly or stability of XRCC1 nuclear foci at sites of oxidative DNA damage. Nucleic Acids Res 2003; 31:5526-33.

45.   Ashworth A. A synthetic lethal therapeutic approach: poly(ADP) ribose polymerase inhibitors for the treatment of cancers deficient in DNA double-strand break repair. J Clin Oncol 2008; 26:3785-90.

46.   Plummer R, Jones C, Middleton M, et al. Phase I study of the poly(ADP-ribose) polymerase inhibitor, AG014699, in combination with temozolomide in patients with advanced solid tumors. Clin Cancer Res 2008; 14:7917-23.

47.   Tumey LN, Bom D, Huck B, et al. The identification and optimization of a N-hydroxy urea series of flap endonuclease 1 inhibitors. Bioorganic & medicinal chemistry letters 2005; 15:277-81.

48.   Luo M, Kelley MR. Inhibition of the human apurinic/apyrimidinic endonuclease (APE1) repair activity and sensitization of breast cancer cells to DNA alkylating agents with lucanthone. Anticancer Res 2004; 24:2127-34.

49.   Fishel ML, He Y, Smith ML, Kelley MR. Manipulation of base excision repair to sensitize ovarian cancer cells to alkylating agent temozolomide. Clin Cancer Res 2007; 13:260-7.

50.   Yan L, Bulgar A, Miao Y, et al. Combined treatment with temozolomide and methoxyamine: blocking apurininc/pyrimidinic site repair coupled with targeting topoisomerase IIalpha. Clin Cancer Res 2007; 13:1532-9.

51.   Trivedi RN, Almeida KH, Fornsaglio JL, Schamus S, Sobol RW. The Role of Base Excision Repair in the Sensitivity and Resistance to Temozolomide Mediated Cell Death. Cancer Res 2005; 65:6394-400.

52.   Trivedi RN, Wang XH, Jelezcova E, Goellner EM, Tang J, Sobol RW. Human methyl purine DNA glycosylase and DNA polymerase ß expression collectively predict sensitivity to temozolomide. Molecular Pharmacology 2008; 74:505-16.

53.   Almeida KH, Sobol RW. A unified view of base excision repair: lesion-dependent protein complexes regulated by post-translational modification. DNA Repair 2007; 6:695-711.

54.   Paik J, Duncan T, Lindahl T, Sedgwick B. Sensitization of human carcinoma cells to alkylating agents by small interfering RNA suppression of 3-alkyladenine-DNA glycosylase. Cancer Res 2005; 65:10472-7.

55.   Sobol RW, Watson DE, Nakamura J, et al. Mutations associated with base excision repair deficiency and methylation-induced genotoxic stress. Proceedings of the National Academy of Science 2002; 99:6860-5.

56.   Liu L, Gerson SL. Therapeutic impact of methoxyamine: blocking repair of abasic sites in the base excision repair pathway. Current Opinion in Investigative Drugs 2004; 5:623-7.

57.   Sobol RW, Horton JK, Kuhn R, et al. Requirement of mammalian DNA polymerase-ß in base-excision repair. Nature 1996; 379:183-6.

58.   Palma JP, Rodriguez LE, Bontcheva-Diaz VD, et al. The PARP inhibitor, ABT-888 potentiates temozolomide: correlation with drug levels and reduction in PARP activity in vivo. Anticancer Res 2008; 28:2625-35.

59.   Liu X, Shi Y, Guan R, et al. Potentiation of temozolomide cytotoxicity by poly(ADP)ribose polymerase inhibitor ABT-888 requires a conversion of single-stranded DNA damages to double-stranded DNA breaks. Mol Cancer Res 2008; 6:1621-9.

60.   Peralta-Leal A, Rodriguez MI, Oliver FJ. Poly(ADP-ribose)polymerase-1 (PARP-1) in carcinogenesis: potential role of PARP inhibitors in cancer treatment. Clin Transl Oncol 2008; 10:318-23.

61.   Hegi ME, Liu L, Herman JG, et al. Correlation of O6-methylguanine methyltransferase (MGMT) promoter methylation with clinical outcomes in glioblastoma and clinical strategies to modulate MGMT activity. J Clin Oncol 2008; 26:4189-99.

62.   Zong WX, Ditsworth D, Bauer DE, Wang ZQ, Thompson CB. Alkylating DNA damage stimulates a regulated form of necrotic cell death. Genes & Development 2004; 18:1272-82.

63.   Cohausz O, Blenn C, Malanga M, Althaus FR. The roles of poly(ADP-ribose)-metabolizing enzymes in alkylation-induced cell death. Cell Mol Life Sci 2008; 65:644-55.

64.   Kolthur-Seetharam U, Dantzer F, McBurney MW, de Murcia G, Sassone-Corsi P. Control of AIF-mediated cell death by the functional interplay of SIRT1 and PARP-1 in response to DNA damage. Cell Cycle 2006; 5:873-7.

65.   Yu SW, Andrabi SA, Wang H, et al. Apoptosis-inducing factor mediates poly(ADP-ribose) (PAR) polymer-induced cell death. Proc Natl Acad Sci U S A 2006; 103:18314-9.

66.   Buelow B, Song Y, Scharenberg AM. The Poly(ADP-ribose) polymerase PARP-1 is required for oxidative stress-induced TRPM2 activation in lymphocytes. J Biol Chem 2008; 283:24571-83.

67.   Fonfria E, Marshall IC, Benham CD, et al. TRPM2 channel opening in response to oxidative stress is dependent on activation of poly(ADP-ribose) polymerase. British journal of pharmacology 2004; 143:186-92.

68.   Formentini L, Macchiarulo A, Cipriani G, et al. Poly(ADP-ribose) catabolism triggers AMP-dependent mitochondrial energy failure. J Biol Chem 2009; 284:17668-76.

69.   Sobol RW, Prasad R, Evenski A, et al. The lyase activity of the DNA repair protein ß-polymerase protects from DNA-damage-induced cytotoxicity. Nature 2000; 405:807-10.

70.   Ochs K, Lips J, Profittlich S, Kaina B. Deficiency in DNA polymerase ß provokes replication-dependent apoptosis via DNA breakage, Bcl-2 decline and caspase-3/9 activation. Cancer Res 2002; 62:1524-30.

71.   Horton JK, Stefanick DF, Wilson SH. Involvement of poly(ADP-ribose) polymerase activity in regulating Chk1-dependent apoptotic cell death. DNA Repair (Amst) 2005; 4:1111-20.

72.   Mrugala MM, Chamberlain MC. Mechanisms of disease: temozolomide and glioblastoma--look to the future. Nat Clin Pract Oncol 2008; 5:476-86.

73.   Tentori L, Graziani G. Recent approaches to improve the antitumor efficacy of temozolomide. Curr Med Chem 2009; 16:245-57.

74.   Sobol RW. Temozolomide. In: Schwab M, editor. Encyclopedia of Cancer. 2nd ed. Berlin, Heidelberg, New York: Springer; 2009.

75.   Wood RD, Mitchell M, Lindahl T. Human DNA repair genes, 2005. Mutat Res 2005; 577:275-83.

76.   Wood RD, Mitchell M, Sgouros J, Lindahl T. Human DNA repair genes. Science 2001; 291:1284-9.

77.   Cahill DP, Levine KK, Betensky RA, et al. Loss of the mismatch repair protein MSH6 in human glioblastomas is associated with tumor progression during temozolomide treatment. Clin Cancer Res 2007; 13:2038-45.

78.   Ranson M, Hersey P, Thompson D, et al. Randomized trial of the combination of lomeguatrib and temozolomide compared with temozolomide alone in chemotherapy naive patients with metastatic cutaneous melanoma. J Clin Oncol 2007; 25:2540-5.

79.   Adhikari S, Choudhury S, Mitra PS, Dubash JJ, Sajankila SP, Roy R. Targeting base excision repair for chemosensitization. Anti-cancer agents in medicinal chemistry 2008; 8:351-7.

80.   Kinsella TJ. Coordination of DNA mismatch repair and base excision repair processing of chemotherapy and radiation damage for targeting resistant cancers. Clin Cancer Res 2009; 15:1853-9.

81.   Chalmers AJ. The potential role and application of PARP inhibitors in cancer treatment. Br Med Bull 2009; 89:23-40.

82.   Tentori L, Leonetti C, Scarsella M, et al. Poly(ADP-ribose) glycohydrolase inhibitor as chemosensitiser of malignant melanoma for temozolomide. Eur J Cancer 2005; 41:2948-57.

83.   Jaiswal AS, Banerjee S, Panda H, et al. A Novel Inhibitor of DNA Polymerase {beta} Enhances the Ability of Temozolomide to Impair the Growth of Colon Cancer Cells. Mol Cancer Res 2009.

84.   Mizushina Y, Manita D, Takeuchi T, et al. The inhibitory action of kohamaic acid A derivatives on mammalian DNA polymerase beta. Molecules 2009; 14:102-21.

85.   Tang J, Goellner EM, Wang XW, et al. Bioenergetic Metabolites Regulate Base Excision Repair-Dependent Cell Death in Response to DNA Damage. Molecular Cancer Research 2010; 8:67-79.

86.   Rosa S, Fortini P, Karran P, Bignami M, Dogliotti E. Processing in vitro of an abasic site reacted with methoxyamine: a new assay for the detection of abasic sites formed in vivo. Nucleic Acids Res 1991; 19:5569-74.

87.   Dantzer F, Ame JC, Schreiber V, Nakamura J, Menissier-de Murcia J, de Murcia G. Poly(ADP-ribose) polymerase-1 activation during DNA damage and repair. Methods Enzymol 2006; 409:493-510.

88.   Fisher AE, Hochegger H, Takeda S, Caldecott KW. Poly(ADP-ribose) polymerase 1 accelerates single-strand break repair in concert with poly(ADP-ribose) glycohydrolase. Mol Cell Biol 2007; 27:5597-605.

89.   Ratnam K, Low JA. Current Development of Clinical Inhibitors of Poly(ADP-Ribose) Polymerase in Oncology. Clin Cancer Res 2007; 13:1383-8.
90.   Cheng CL, Johnson SP, Keir ST, et al. Poly(ADP-ribose) polymerase-1 inhibition reverses temozolomide resistance in a DNA mismatch repair-deficient malignant glioma xenograft. Mol Cancer Ther 2005; 4:1364-8.
91.   Tentori L, Leonetti C, Scarsella M, et al. Systemic administration of GPI 15427, a novel poly(ADP-ribose) polymerase-1 inhibitor, increases the antitumor activity of temozolomide against intracranial melanoma, glioma, lymphoma. Clinical Cancer Research 2003; 9:5370-9.
92.   Tentori L, Portarena I, Torino F, Scerrati M, Navarra P, Graziani G. Poly(ADP-ribose) polymerase inhibitor increases growth inhibition and reduces G(2)/M cell accumulation induced by temozolomide in malignant glioma cells. Glia 2002; 40:44-54.
93.   Tentori L, Portarena I, Vernole P, et al. Effects of single or split exposure of leukemic cells to temozolomide, combined with poly(ADP-ribose) polymerase inhibitors on cell growth, chromosomal aberrations and base excision repair components. Cancer Chemotherapy & Pharmacology 2001; 47:361-9.
94.   Miknyoczki SJ, Jones-Bolin S, Pritchard S, et al. Chemopotentiation of temozolomide, irinotecan, and cisplatin activity by CEP-6800, a poly(ADP-ribose) polymerase inhibitor. Mol Cancer Ther 2003; 2:371-82.
95.   Calabrese CR, Almassy R, Barton S, et al. Anticancer chemosensitization and radiosensitization by the novel poly(ADP-ribose) polymerase-1 inhibitor AG14361. J Natl Cancer Inst 2004; 96:56-67.
96.   Calabrese CR, Batey MA, Thomas HD, et al. Identification of potent nontoxic poly(ADP-Ribose) polymerase-1 inhibitors: chemopotentiation and pharmacological studies. Clin Cancer Res 2003; 9:2711-8.
97.   Curtin NJ, Wang LZ, Yiakouvaki A, et al. Novel poly(ADP-ribose) polymerase-1 inhibitor, AG14361, restores sensitivity to temozolomide in mismatch repair-deficient cells. Clin Cancer Res 2004; 10:881-9.
98.   Palma JP, Wang YC, Rodriguez LE, et al. ABT-888 Confers Broad In vivo Activity in Combination with Temozolomide in Diverse Tumors. Clin Cancer Res 2009.
99.   Koh DW, Lawler AM, Poitras MF, et al. Failure to degrade poly(ADP-ribose) causes increased sensitivity to cytotoxicity and early embryonic lethality. Proc Natl Acad Sci U S A 2004; 101:17699-704.
100.   Cortes U, Tong WM, Coyle DL, et al. Depletion of the 110-kilodalton isoform of poly(ADP-ribose) glycohydrolase increases sensitivity to genotoxic and endotoxic stress in mice. Mol Cell Biol 2004; 24:7163-78.
101.   Rinne M, Caldwell D, Kelley MR. Transient adenoviral N-methylpurine DNA glycosylase overexpression imparts chemotherapeutic sensitivity to human breast cancer cells. Mol Cancer Ther 2004; 3:955-67.
102.   Wang D, Zhong ZY, Zhang QH, Li ZP, Kelley MR. [Effect of adenoviral N-methylpurine DNA glycosylase overexpression on chemosensitivity of human osteosarcoma cells]. Zhonghua Bing Li Xue Za Zhi 2006; 35:352-6.
103.   Poeschla EM, Wong-Staal F, Looney DJ. Efficient transduction of nondividing human cells by feline immunodeficiency virus lentiviral vectors. Nat Med 1998; 4:354-7.
104.   Zufferey R, Dull T, Mandel RJ, et al. Self-inactivating lentivirus vector for safe and efficient in vivo gene delivery. J Virol 1998; 72:9873-80.

105.   Zufferey R, Nagy D, Mandel RJ, Naldini L, Trono D. Multiply attenuated lentiviral vector achieves efficient gene delivery in vivo. Nat Biotechnol 1997; 15:871-5.

106.   Park MJ, Kim MS, Park IC, et al. PTEN suppresses hyaluronic acid-induced matrix metalloproteinase-9 expression in U87MG glioblastoma cells through focal adhesion kinase dephosphorylation. Cancer Res 2002; 62:6318-22.

107.   Ishii N, Maier D, Merlo A, et al. Frequent co-alterations of TP53, p16/CDKN2A, p14ARF, PTEN tumor suppressor genes in human glioma cell lines. Brain Pathol 1999; 9:469-79.

108.   Parsons JL, Tait PS, Finch D, et al. Ubiquitin ligase ARF-BP1/Mule modulates base excision repair. EMBO J 2009; 28:3207-15.

109.   Palumbo R, Sampaolesi M, De Marchis F, et al. Extracellular HMGB1, a signal of tissue damage, induces mesoangioblast migration and proliferation. J Cell Biol 2004; 164:441-9.

110.   Yu J, Wang P, Ming L, Wood MA, Zhang L. SMAC/Diablo mediates the proapoptotic function of PUMA by regulating PUMA-induced mitochondrial events. Oncogene 2007; 26:4189-98.

111.   Meira LB, Moroski-Erkul CA, Green SL, et al. Aag-initiated base excision repair drives alkylation-induced retinal degeneration in mice. Proc Natl Acad Sci U S A 2009; 106:888-93.

112.   Roth RB, Samson LD. 3-Methyladenine DNA glycosylase-deficient Aag null mice display unexpected bone marrow alkylation resistance. Cancer Res 2002; 62:656-60.

113.   Engelward BP, Dreslin A, Christensen J, Huszar D, Kurahara C, Samson L. Repair-deficient 3-methyladenine DNA glycosylase homozygous mutant mouse cells have increased sensitivity to alkylation-induced chromosome damage and cell killing. EMBO Journal 1996; 15:945-52.

114.   Eliasson MJ, Sampei K, Mandir AS, et al. Poly(ADP-ribose) polymerase gene disruption renders mice resistant to cerebral ischemia. Nat Med 1997; 3:1089-95.

115.   Endres M, Wang ZQ, Namura S, Waeber C, Moskowitz MA. Ischemic brain injury is mediated by the activation of poly(ADP-ribose)polymerase. J Cereb Blood Flow Metab 1997; 17:1143-51.

116.   Sobol RW, Kartalou M, Almeida KH, et al. Base Excision Repair Intermediates Induce p53-independent Cytotoxic and Genotoxic Responses. J Biol Chem 2003; 278:39951-9.

117.   Kanzawa T, Germano IM, Komata T, Ito H, Kondo Y, Kondo S. Role of autophagy in temozolomide-induced cytotoxicity for malignant glioma cells. Cell Death Differ 2004; 11:448-57.

118.   Lotze MT, Tracey KJ. High-mobility group box 1 protein (HMGB1): nuclear weapon in the immune arsenal. Nature reviews 2005; 5:331-42.

119.   Ditsworth D, Zong WX, Thompson CB. Activation of poly(ADP)-ribose polymerase (PARP-1) induces release of the pro-inflammatory mediator HMGB1 from the nucleus. J Biol Chem 2007; 282:17845-54.

120.   Prasad R, Liu Y, Deterding LJ, et al. HMGB1 is a cofactor in mammalian base excision repair. Mol Cell 2007; 27:829-41.

121.   Xu Y, Huang S, Liu ZG, Han J. Poly(ADP-ribose) polymerase-1 signaling to mitochondria in necrotic cell death requires RIP1/TRAF2-mediated JNK1 activation. J Biol Chem 2006; 281:8788-95.

122.   Festjens N, Vanden Berghe T, Cornelis S, Vandenabeele P. RIP1, a kinase on the crossroads of a cell's decision to live or die. Cell Death Differ 2007; 14:400-10.

123. Hur GM, Kim YS, Won M, Choksi S, Liu ZG. The death domain kinase RIP has an important role in DNA damage-induced, p53-independent cell death. J Biol Chem 2006; 281:25011-7.

124. Temkin V, Huang Q, Liu H, Osada H, Pope RM. Inhibition of ADP/ATP exchange in receptor-interacting protein-mediated necrosis. Mol Cell Biol 2006; 26:2215-25.

125. Xu X, Chua CC, Kong J, et al. Necrostatin-1 protects against glutamate-induced glutathione depletion and caspase-independent cell death in HT-22 cells. J Neurochem 2007; 103:2004-14.

126. Degterev A, Hitomi J, Germscheid M, et al. Identification of RIP1 kinase as a specific cellular target of necrostatins. Nat Chem Biol 2008; 4:313-21.

127. Bonicalzi ME, Haince JF, Droit A, Poirier GG. Regulation of poly(ADP-ribose) metabolism by poly(ADP-ribose) glycohydrolase: where and when? Cell Mol Life Sci 2005; 62:739-50.

128. Dumitriu IE, Voll RE, Kolowos W, et al. UV irradiation inhibits ABC transporters via generation of ADP-ribose by concerted action of poly(ADP-ribose) polymerase-1 and glycohydrolase. Cell Death Differ 2004; 11:314-20.

129. Bentle MS, Reinicke KE, Bey EA, Spitz DR, Boothman DA. Calcium-dependent modulation of poly(ADP-ribose) polymerase-1 alters cellular metabolism and DNA repair. J Biol Chem 2006; 281:33684-96.

130. Bey EA, Bentle MS, Reinicke KE, et al. An NQO1- and PARP-1-mediated cell death pathway induced in non-small-cell lung cancer cells by beta-lapachone. Proc Natl Acad Sci U S A 2007; 104:11832-7.

131. Heeres JT, Hergenrother PJ. Poly(ADP-ribose) makes a date with death. Curr Opin Chem Biol 2007; 11:644-53.

132. Andrabi SA, Kim NS, Yu SW, et al. Poly(ADP-ribose) (PAR) polymer is a death signal. Proc Natl Acad Sci U S A 2006; 103:18308-13.

133. Berger NA. Poly(ADP-ribose) in the cellular response to DNA damage. Radiat Res 1985; 101:4-15.

134. Berger NA, Sims JL, Catino DM, Berger SJ. Poly(ADP-ribose) polymerase mediates the suicide response to massive DNA damage: studies in normal and DNA-repair defective cells. Princess Takamatsu Symp 1983; 13:219-26.

135. Jacobson MK, Levi V, Juarez-Salinas H, Barton RA, Jacobson EL. Effect of carcinogenic N-alkyl-N-nitroso compounds on nicotinamide adenine dinucleotide metabolism. Cancer Res 1980; 40:1797-802.

136. Formentini L, Moroni F, Chiarugi A. Detection and pharmacological modulation of nicotinamide mononucleotide (NMN) in vitro and in vivo. Biochemical pharmacology 2009; 77:1612-20.

137. Hasmann M, Schemainda I. FK866, a highly specific noncompetitive inhibitor of nicotinamide phosphoribosyltransferase, represents a novel mechanism for induction of tumor cell apoptosis. Cancer Res 2003; 63:7436-42.

138. Maksimenko A, Ishchenko AA, Sanz G, Laval J, Elder RH, Saparbaev MK. A molecular beacon assay for measuring base excision repair activities. Biochem Biophys Res Commun 2004; 319:240-6.

139. Connor EE, Wilson JJ, Wyatt MD. Effects of substrate specificity on initiating the base excision repair of N-methylpurines by variant human 3-methyladenine DNA glycosylases. Chem Res Toxicol 2005; 18:87-94.

140. Sobol RW, Kartalou M, Almeida KH, et al. Base excision repair intermediates induce p53-independent cytotoxic and genotoxic responses. J Biol Chem 2003; 278:39951-9.

141. Sobol RW, Horton JK, Kuhn R, et al. Requirement of mammalian DNA polymerase-beta in base-excision repair. Nature 1996; 379:183-6.

142. Sobol RW, Prasad R, Evenski A, et al. The lyase activity of the DNA repair protein beta-polymerase protects from DNA-damage-induced cytotoxicity. Nature 2000; 405:807-10.

143. Stein GH. T98G: an anchorage-independent human tumor cell line that exhibits stationary phase G1 arrest in vitro. Journal of cellular physiology 1979; 99:43-54.

144. Donawho CK, Luo Y, Penning TD, et al. ABT-888, an orally active poly(ADP-ribose) polymerase inhibitor that potentiates DNA-damaging agents in preclinical tumor models. Clin Cancer Res 2007; 13:2728-37.

145. Kauppinen TM, Chan WY, Suh SW, Wiggins AK, Huang EJ, Swanson RA. Direct phosphorylation and regulation of poly(ADP-ribose) polymerase-1 by extracellular signal-regulated kinases 1/2. Proc Natl Acad Sci U S A 2006; 103:7136-41.

146. Rajamohan SB, Pillai VB, Gupta M, et al. SIRT1 promotes cell survival under stress by deacetylation-dependent deactivation of poly(ADP-ribose) polymerase 1. Mol Cell Biol 2009; 29:4116-29.

147. Moubarak RS, Yuste VJ, Artus C, et al. Sequential activation of poly(ADP-ribose) polymerase 1, calpains, and Bax is essential in apoptosis-inducing factor-mediated programmed necrosis. Mol Cell Biol 2007; 27:4844-62.

148. Hofseth LJ, Khan MA, Ambrose M, et al. The adaptive imbalance in base excision-repair enzymes generates microsatellite instability in chronic inflammation. Journal of Clinical Investigation 2003; 112:1887-94.

149. Wang Y, Kim NS, Li X, et al. Calpain activation is not required for AIF translocation in PARP-1-dependent cell death (parthanatos). J Neurochem 2009; 110:687-96.

150. Ethier C, Labelle Y, Poirier GG. PARP-1-induced cell death through inhibition of the MEK/ERK pathway in MNNG-treated HeLa cells. Apoptosis 2007; 12:2037-49.

151. LeDoux SP, Wilson GL, Beecham EJ, Stevnsner T, Wassermann K, Bohr VA. Repair of mitochondrial DNA after various types of DNA damage in Chinese hamster ovary cells. Carcinogenesis 1992; 13:1967-73.

152. Huang Q, Wu YT, Tan HL, Ong CN, Shen HM. A novel function of poly(ADP-ribose) polymerase-1 in modulation of autophagy and necrosis under oxidative stress. Cell Death Differ 2009; 16:264-77.

153. Dali-Youcef N, Lagouge M, Froelich S, Koehl C, Schoonjans K, Auwerx J. Sirtuins: the 'magnificent seven', function, metabolism and longevity. Annals of medicine 2007; 39:335-45.

154. Berger F, Lau C, Dahlmann M, Ziegler M. Subcellular compartmentation and differential catalytic properties of the three human nicotinamide mononucleotide adenylyltransferase isoforms. J Biol Chem 2005; 280:36334-41.

155. Pieper AA, Walles T, Wei G, et al. Myocardial postischemic injury is reduced by polyADPribose polymerase-1 gene disruption. Mol Med 2000; 6:271-82.

156. Ha HC, Snyder SH. Poly(ADP-ribose) polymerase is a mediator of necrotic cell death by ATP depletion. Proc Natl Acad Sci U S A 1999; 96:13978-82.

157. Wang S, Xing Z, Vosler PS, et al. Cellular NAD replenishment confers marked neuroprotection against ischemic cell death: role of enhanced DNA repair. Stroke 2008; 39:2587-95.

158.   Liu D, Gharavi R, Pitta M, Gleichmann M, Mattson MP. Nicotinamide prevents NAD+ depletion and protects neurons against excitotoxicity and cerebral ischemia: NAD+ consumption by SIRT1 may endanger energetically compromised neurons. Neuromolecular Med 2009; 11:28-42.

159.   Masutani M, Suzuki H, Kamada N, et al. Poly(ADP-ribose) polymerase gene disruption conferred mice resistant to streptozotocin-induced diabetes. Proc Natl Acad Sci U S A 1999; 96:2301-4.

160.   Cardinal JW, Margison GP, Mynett KJ, Yates AP, Cameron DP, Elder RH. Increased susceptibility to streptozotocin-induced beta-cell apoptosis and delayed autoimmune diabetes in alkylpurine-DNA-N-glycosylase-deficient mice. Mol Cell Biol 2001; 21:5605-13.

161.   Burns N, Gold B. The effect of 3-methyladenine DNA glycosylase-mediated DNA repair on the induction of toxicity and diabetes by the beta-cell toxicant streptozotocin. Toxicol Sci 2007; 95:391-400.

162.   Pieper AA, Brat DJ, Krug DK, et al. Poly(ADP-ribose) polymerase-deficient mice are protected from streptozotocin-induced diabetes. Proc Natl Acad Sci U S A 1999; 96:3059-64.

163.   Garten A, Petzold S, Korner A, Imai S, Kiess W. Nampt: linking NAD biology, metabolism and cancer. Trends Endocrinol Metab 2009; 20:130-8.

164.   Cerda SR, Turk PW, Thor AD, Weitzman SA. Altered expression of the DNA repair protein, N-methylpurine-DNA glycosylase (MPG) in breast cancer. FEBS Lett 1998; 431:12-8.

165.   Kim NK, Ahn JY, Song J, et al. Expression of the DNA repair enzyme, N-methylpurine-DNA glycosylase (MPG) in astrocytic tumors. Anticancer Res 2003; 23:1417-23.

166.   Bryant HE, Schultz N, Thomas HD, et al. Specific killing of BRCA2-deficient tumours with inhibitors of poly(ADP-ribose) polymerase. Nature 2005; 434:913-7.

167.   Farmer H, McCabe N, Lord CJ, et al. Targeting the DNA repair defect in BRCA mutant cells as a therapeutic strategy. Nature 2005; 434:917-21.